There are amendments to this paper

Dissecting and rebuilding the glioblastoma microenvironment with engineered materials

Kayla J. Wolf[1,2], *Joseph Chen*[2], *Jason D. Coombes*[2,3], *Manish K. Aghi*[4] *and Sanjay Kumar*[1,2,5]*

Abstract | Glioblastoma (GBM) is the most aggressive and common form of primary brain cancer. Several decades of research have provided great insight into GBM progression; however, the prognosis remains poor, with a median patient survival time of ~15 months. The tumour microenvironment (TME) of GBM plays a crucial role in mediating tumour progression and thus is being explored as a therapeutic target. Progress in the development of treatments targeting the TME is currently limited by a lack of model systems that can accurately recreate the distinct extracellular matrix composition and anatomic features of the brain, such as the blood–brain barrier and axonal tracts. Biomaterials can be applied to develop synthetic models of the GBM TME to mimic physiological and pathophysiological features of the brain, including cellular and extracellular matrix composition, mechanical properties and topography. In this Review, we summarize key features of the GBM microenvironment and discuss different strategies for the engineering of GBM TME models, including 2D and 3D models featuring chemical and mechanical gradients, interfaces and fluid flow. Finally, we highlight the potential of engineered TME models as platforms for mechanistic discovery and drug screening, as well as preclinical testing and precision medicine.

[1]*University of California, Berkeley–University of California, San Francisco Graduate Program in Bioengineering, Berkeley, CA, USA.*

[2]*Department of Bioengineering, University of California, Berkeley, Berkeley, CA, USA.*

[3]*Department of Inflammation Biology, Faculty of Life Sciences and Medicine, King's College London, London, UK.*

[4]*Department of Neurosurgery, University of California, San Francisco (UCSF), San Francisco, CA, USA.*

[5]*Department of Chemical and Biomolecular Engineering, University of California, Berkeley, Berkeley, CA, USA.*

**e-mail: skumar@berkeley.edu*

https://doi.org/10.1038/s41578-019-0135-y

Glioblastoma (GBM) is the most common and aggressive primary central nervous system tumour, with a devastatingly low median patient survival of 15 months[1,2] (BOX 1). Standard treatment consists of surgical resection, followed by chemotherapy and radiotherapy[3]. However, GBMs exhibit a diffuse invasion pattern, in which tumour cells either migrate individually or collectively infiltrate healthy tissue beyond the tumour margin[4], making complete surgical resection virtually impossible[5]. Radiotherapy protocols cover a 2 cm margin beyond the visible tumour margin; however, microscopic tumour invasion may spread beyond this distance[6]. Infiltrating tumour cells are enriched with glioblastoma stem cells (GSCs), which are tumour cells characterized by their ability to recapitulate the vast heterogeneity of GBM cell phenotypes through propagation and differentiation[7]. GSCs are often highly refractory to chemotherapy, driving tumour recurrence and chemoresistance[8]. The tumour microenvironment (TME), which contains extracellular matrix (ECM), interstitial fluid and various stromal cells (for example, astrocytes, macrophages and endothelial cells), is a key regulator of tumour progression[9]. Substantial advances have already been made in understanding microenvironmental contributions to the progression of other cancers, particularly breast cancer[10–13] and pancreatic cancer[14,15]. Therefore, new therapies have also been developed to target the GBM TME[16,17].

Unique features of the brain TME include the blood–brain barrier (BBB), the presence of myelinated and interconnected axon tracts, and a distinct ECM composition, all of which pose specific challenges for treatment[9,18,19]. The BBB, even after losing integrity during tumour progression, is impassable for most chemotherapeutics[20] and is especially impermeable in the actively invading tumour regions, where the BBB is intact[21]. Haptotactic cues from the vascular basement membrane and enrichment of vascular-derived chemotactic cues further drive cell invasion and therapeutic resistance of tumour cells in the perivascular space[18]. Interconnected axon tracts also provide haptotactic cues for cellular invasion and represent a major barrier to surgical resection[22,23]. Furthermore, in contrast to other solid tissues, brain ECM is particularly soft (300–3,000 Pa)[24,25], lacks collagen fibres and is rich in hyaluronic acid (HA), tenascins and chondroitin sulfates[19]. Interestingly, GBMs

Box 1 | **Clinical overview of glioblastoma**

Glioblastoma (GBM) comprises 47.7% of all malignant primary central nervous system tumours, with a 5-year patient survival of 5.6%[1]. About 95% of patients are diagnosed after 40 years of age (median age = 65 years) and no genetic predispositions are known[256]. GBM driver mutations can be traced to astrocyte-like neural stem cells in the subventricular zone[257]; notably, targeting radiotherapy towards the subventricular zone improves patient outcome[258,259]. Primary GBM tumours arise de novo and account for 90% of cases, whereas secondary tumours arise from lower-grade gliomas and account for 10% of cases[260]. Secondary tumours are typically diagnosed in younger patients (mean age = 45 years) and correlate with longer survival[1,260]. Patients with both primary and secondary tumours typically present symptoms of increased intracranial pressure, such as headaches, neurological defects and seizures[109]. The diagnosis of GBM is based on the presence of several histological features, including anaplasia, mitotic activity, microvascular proliferation and necrosis[261]. Isocitrate dehydrogenase (IDH) mutant status correlates with secondary GBM and better prognosis, possibly because IDH mutation increases genome-wide methylation[262,263].

Standard treatment is surgical resection, followed by chemotherapy and radiation[3]. Surgical resection provides clinical relief, enables tissue acquisition for diagnostic analysis and increases survival[5]. However, complete surgical resection is virtually impossible and must be balanced with preserving intact tissue[264]. Since 2005, the alkylating agent temozolomide (TMZ) combined with radiotherapy has become the standard of care for newly diagnosed GBM[3,265]. Methylation of the promoter necessary to express O^6-methylguanine methyltransferase, a DNA excision repair enzyme, suppresses reversal of TMZ-induced DNA damage and correlates with increased survival[266]. Despite initial efficacy, tumours ultimately acquire therapeutic resistance and recur[8]. Nitrosoureas or a combination of procarbazine, lomustine and vincristine are second-line treatments, owing to their higher toxicity and poorer efficacy compared with TMZ[267,268]. Bevacizumab, an antibody-based antiangiogenic therapy, which normalizes the vasculature, was approved by the US Food and Drug Administration (FDA) for recurrent GBM in 2009, but was ultimately ineffective at treating GBM in randomized clinical trials[99,151–153]. Steroids, specifically dexamethasone, are prescribed throughout treatment to ameliorate peritumoural oedema and discomfort[5].

rarely intravasate and metastasize from the brain, possibly owing to early patient mortality or the unique features of the brain TME[26].

Investigations of TME–tumour interactions are limited by a lack of model systems that accurately represent the human brain microenvironment. Biomaterials and engineered devices offer the possibility to recreate brain-like TMEs, enabling mechanistic discovery and therapeutic screening in environments that mimic tissue more closely than traditional 2D culture paradigms. For example, standard tissue culture plastic and reconstituted basement membrane preparations lack design flexibility and fail to capture key compositional, structural and mechanical features of the brain TME[27–29]. Furthermore, engineered TME models can be tailored to incorporate patient-derived cells and matrix, offering a route towards precision medicine. In this Review, we summarize how the TME drives GBM progression, describe potential therapeutic targets and investigate designs and applications of engineered TME models in research and the clinic. Finally, we outline new directions for designing, fabricating and employing engineered models in patient care.

Glioblastoma microenvironment

The TME provides a dynamic array of signals that drive proliferation, invasion and resistance (FIG. 1). These signals can be broadly categorized into ECM composition, ECM mechanics, topographical cues, interstitial fluid and stromal-cell interactions (TABLE 1).

Extracellular matrix. Normal brain ECM, in contrast to the ECM of other solid tissues, is enriched in glycoproteins, such as tenascins and link proteins, glycosaminoglycans (GAGs), such as HA, and proteoglycans, such as aggrecan, neurocan, versican and phosphacan[30]. Conversely, fibrillar proteins, such as collagen and fibronectin, are relatively sparse[31]. In tumours, the abundance of ECM components is altered; in particular, the level of GAGs is increased by 3–4-fold[32]. Astrocytes and oligodendrocytes produce the majority of brain ECM in normal tissue, but GBM cells also express their own pro-invasive matrix[18,33]. GBM cells can also induce stromal cells to express specific ECM components. In highly angiogenic tumours, tumour cells overexpress tenascins and vitronectin, and stromal cells produce excess laminin, fibronectin and collagen IV[34].

HA, a polyanionic GAG localized primarily in the intraparenchymal region, is the most abundant component of brain ECM[31]. Expressed as a megadalton linear chain in healthy tissue, HA regulates tissue mechanics, organization and hydration. HA also activates cellular signalling through surface receptors such as CD44 and receptor for hyaluronan-mediated motility (RHAMM)[35,36]. The differential signal transduction and functional contributions of CD44 and RHAMM remain incompletely understood; however, it is known that both receptors can drive invasion[37–39]. Both tumour and stromal cells produce HA in high-grade gliomas and GBMs overexpress hyaluronan synthase 2 (HAS2)[40–42]. Whether downstream signals arising from HA–receptor interactions are pathologic is determined by the molecular weight of HA; low-molecular-weight HA provides pro-invasive cues and high-molecular-weight HA reduces tumour invasion[43,44]. Accordingly, GBM spheroids are less invasive in 3D matrices cross-linked with 500 kDa HA than with 60 kDa or 10 kDa HA[45]. The crucial role of HA in GBM progression motivates the investigation of the effects of the molecular weight, mechanical properties and signalling of HA in engineered TME models.

Laminin, fibronectin and collagen IV are mainly localized in vascular basement membranes[19,46]. Laminin has been shown to be particularly potent in driving GBM progression; however, downstream signalling mechanisms may be isoform specific[47]. For example, in a zebrafish model, laminin α5 increases the formation of blood-vessel-dependent tumours but reduces the migration speed of GBM cells[48]. In human cell culture models, laminin α2 supports GSC growth[49]. Interestingly, GSCs are often propagated on laminin-coated culture dishes, and laminin-binding integrin α6 is necessary for GSC renewal, proliferation and tumour formation[50]. By contrast, fibronectin expression is often decreased in GBMs[51]. Fibronectin assembly reduces GBM cell migration and fibronectin depletion increases migration[52,53]. Pharmacological disruption of fibronectin assembly in orthotopic mouse models also sensitizes tumours to chemotherapy[54]. Thus, assembled fibronectin may inhibit GBM cell invasion but may also reduce the efficacy of chemotherapy. Whether targeted disruption of fibronectin would advance or counteract therapeutic goals remains unclear. Fibrillar collagens,

such as collagen I, are not abundant in normal brain tissue; however, non-fibrillar collagen IV is present in basement membranes of the brain vasculature[55,56]. Despite widespread use in engineered TME models[27,29], the role of parenchymal collagen in GBMs in vivo is unclear. Evidence suggests that the structural organization of collagen has an influence on GBMs; accumulation of punctate or non-fibrillar collagen can be correlated with a

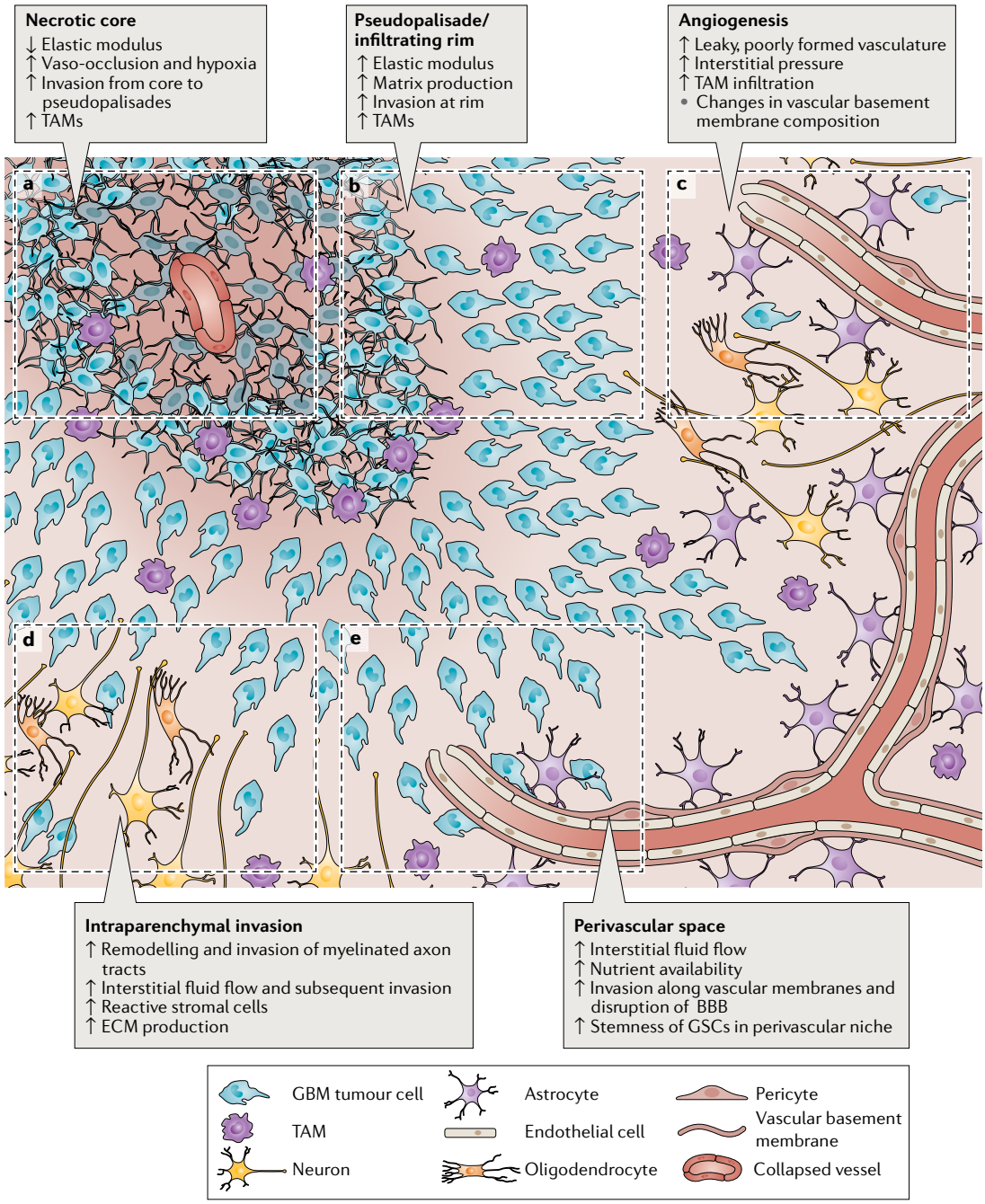

Fig. 1 | **Schematic of glioblastoma regions.** This glioblastoma (GBM) schematic illustrates changes during tumour progression in the different microenvironmental regions. **a** | The necrotic core is softer than surrounding tissue and is thought to form after increases in cell density beyond a certain threshold or vaso-occlusive events result in hypoxia. **b** | Pseudopalisades are regions of high cell density thought to form as cells migrate away from hypoxic regions. These zones have an increased elastic modulus and matrix production compared with healthy tissue and necrotic regions. GBM cells invade from the outer edge of the cell-dense tumour into healthy tissue at the infiltrating rim. **c** | GBM tumours show hypervascularity with increased angiogenesis compared with healthy brain tissue. Tumour-associated vasculature is poorly formed, leaky and leads to an increase in interstitial fluid pressure. **d** | Tumour cells invading through the parenchyma often follow and remodel the surface of myelinated tracts — a region in which high interstitial fluid flow may also drive invasion. **e** | Tumour cells rapidly invade the vasculature, where they are exposed to nutrients, high interstitial fluid flow and haptotactic cues in basement membranes. The perivascular niche also supports stemness and survival of glioblastoma stem cells (GSCs). BBB, blood–brain barrier; ECM, extracellular matrix; TAM, tumour-associated macrophage.

Table 1 | **Key signals in the tumour microenvironment**

Signal type	Signal	Signalling effects	Effect on tumour progression	Refs
Matrix composition	HA	GBM cells increase HA synthesis and degradation	Low MW HA accumulates and promotes GBM cell invasion, GSC stemness and GSC resistance	31,37–45
	Fibronectin	GBM cells decrease fibronectin expression and crosslinking	Invasion and sensitivity to therapy increase	51–54
	Tenascin C	GBM cells express more tenascin C	Tenascin C increases matrix stiffness and GBM cell invasion and proliferation	60–62
	Laminin	GSCs interact with laminin	GSCs show increased stemness, invasion and proliferation	48–51
Matrix mechanics	Elastic modulus	Elastic modulus increases in pseudopalisades and decreases in necrotic core compared with healthy tissue	Increased modulus promotes GBM cell migration and proliferation in vitro	69–75,77,78
	Density	GBM cells produce more matrix than non-tumour cells	High matrix density decreases perfusion and increases ECM compaction and cell damage	79,80
Topography	Microvasculature	Tumours exhibit hypervascularity with loss of BBB integrity and change in basement membrane composition	Tumour cells invade rapidly along vasculature	63,64
	Myelinated tracts	GBM cells remodel myelin coating	GBM cells invade rapidly along myelinated tracts	84–88
Interstitial fluid	Pressure	Tumours exhibit oedema	Pressure from oedema is a barrier to chemotherapy	91,92
	Fluid flow	Convection-enhanced therapy increases flow rates	Fluid flow promotes invasion and proliferation	93–97,170
Stromal and endothelial cell crosstalk	TAMs	GBM-derived osteopontin recruits and maintains TAM phenotype; TAMs secrete a complex array of cytokines and growth factors	Immune activity (from cytotoxic T cells) increases; growth factors increase GBM proliferation, survival and migration	103,104
	TAAs	GBM cells activate TAAs; TAAs activate tumour cell MMP and uPA expression	Intratumoural immune response decreases; GBM invasion increases and cells become more chemoresistant	102
	Vascular endothelial cells	Vascular endothelial cells secrete IL-8	GSC migration, proliferation and stemness increase	106
	Neurons	Neurons secrete neuroligin-3	GBM proliferation increases	105
	MSCs	MSCs provide exosome cargo such as miR-1587 and secrete IL-6	GSCs proliferation and tumour cell survival increase	100,101

BBB, blood–brain barrier; ECM, extracellular matrix; GBM, glioblastoma; GSC, glioblastoma stem cell; HA, hyaluronic acid; IL, interleukin; miR, microRNA; MMP, matrix metalloprotease; MSC, mesenchymal stem cell; MW, molecular weight; TAA, tumour-associated astrocyte; TAM, tumour-associated macrophage; uPA, urokinase-type plasminogen activator.

more invasive phenotype than accumulation of organized fibrillar collagen, which may structurally impede parenchymal invasion[57].

The brain also contains matricellular proteins, which regulate tissue structure and tumour invasion[30]. Tenascin C, which is a large (180–250 kDa) glycoprotein that crosslinks matrix, is particularly important in GBM progression[58,59]. Aggressive gliomas are enriched in tenascin C, which correlates with poorer patient prognosis[60]. Interestingly, glioma ECM stiffness also corresponds with levels of tenascin C but not with levels of type I collagen abundance, vascularity or tumour cell density[60]. Tenascin C further participates in cell–cell crosstalk. Tumour-cell-derived tenascin C interacts with α5β1 and αvβ6 integrins on T lymphocytes, resulting in reduced mTOR signalling and immunosuppression[61]. Additionally, the presence of tenascin C in collagen I matrices leads to an increase in matrix metalloproteinase (MMP)-12-mediated GBM invasion[62]. Other matricellular proteins, notably agrin, insulin-like growth factor-binding protein (IGFBP) 7 and secreted protein acidic and rich in cysteine (SPARC), are dysregulated in GBM vascular basement membranes, which may contribute to the disruption of the BBB and angiogenesis[63,64]. The matricellular protein osteopontin (*Spp1*) is further implicated in promoting GBM therapeutic resistance. Osteopontin affects the permissiveness of the TME and maintains the stemness of GSCs through CD44-dependent signalling in the perivascular space[65–67].

The expression of these different ECM components is highly intertwined. For example, silencing uridine diphosphate-glucose 6-dehydrogenase (UGDH), which is an enzyme required for GAG monomer synthesis, results in decreased GAG production and abundance of tenascin C and brevican, leading to a reduction of tumour growth and migration in animal models[68]. Therefore, dissecting the complexity of matrix composition in engineered TME models may uncover targetable drivers of GBM progression.

The mechanical properties of the tumour ECM, for example, matrix density and bulk storage modulus, also

play an important role in GBM progression. Like most tumours, GBMs also exhibit an elastic modulus almost twice that of normal tissue, possibly owing to changes in ECM expression and increased compaction[69,70]. However, the elastic modulus varies strongly by region, with a lower modulus observed in necrotic regions (~0.1 kPa) than in the hypercellular core (~10 kPa) and a higher modulus observed in the hypercellular core compared with healthy tissue (1 kPa)[71]. Notably, GBM cell proliferation and migration is mechanosensitive[72,73], although the degree of mechanosensitivity varies between patients[74]. The mechanosensitivity also differs between tumour cell subpopulations, and some GSCs lack mechanosensitivity[75,76]. High matrix modulus (6.9 kPa compared with 0.15 kPa) induces CD44-dependent cell migration and spreading on HA[77]. High matrix modulus (119 kPa compared with 0.08 kPa) also amplifies epidermal growth factor receptor (EGFR) signalling, promoting proliferation[78]. Matrix density is also higher in GBMs than in healthy brain tissue, perhaps owing to compaction caused by matrix overexpression and high cell density. Compaction of GBM cells in vitro further induces expression of collagen IV and VI, vascular endothelial growth factor (VEGF) and the collagen-crosslinking enzyme lysyl oxidase, which is associated with an increase in angiogenesis and matrix elastic modulus[79]. The growing tumour mechanically compresses tissue, damaging neurons and restricting vascular perfusion[80]. GBM ECM remodelling progresses as a positive feedback loop in which tumour cell proliferation and ECM production cause an increase in elastic modulus, which, in turn, further promotes tumour cell proliferation and invasion.

Tumour–stroma interactions. GBM cells most rapidly invade along anatomical tracks, such as the vasculature and myelinated axons[19,23] (FIG. 1c,d,e). As GBM cells invade through the perivascular space along the vascular basement membrane, they disrupt astrocytic end feet contacts with endothelial cells and weaken the BBB[81] (FIG. 1e). A combination of haptotactic, chemotactic and topographic cues are likely responsible for this pattern of invasion. Many integrin-binding matrix proteins, such as laminin, collagen and fibronectin, are localized at the vascular basement membrane and are relatively sparse in other brain regions[19,46]. Basement membranes have a higher elastic modulus than the surrounding matrix, which may promote a mechanosensitive, integrin-mediated migration[82]. The perivascular space is also rich in paracrine signals from perivascular support cells, as well as nutrients crossing the BBB[83]. The detailed mechanisms of invasion along myelinated axon tracts remain elusive thus far; however, MMP-mediated remodelling of myelin from a non-adhesive to an adhesive substrate is likely involved[84–87]. GSCs that migrate along remodelled or deteriorating white-matter tracts gain access to the Notch ligand Jagged1 on exposed nerve fibres, which further promotes invasive growth[88]. Culturing GBM cells on engineered surfaces with linear topographies shows that linear presentation of ECM cues strongly affects migration speed. The resulting constraint and alignment of actin bundles, as well as cytoskeletal polymerization, coordinate rapid, persistent migration[89,90].

Solid tumours exhibit an abnormally high interstitial fluid pressure and volume, mainly owing to leaky vasculature[91,92]. Interstitial fluid flow is most rapid along axon tracts and in perivascular spaces, promoting the distribution of soluble cues, for example, pro-angiogenic factors[93]. Rapid flow in parallel with white-matter tracts leads to an increase in the invasion speed of tumour cells, possibly owing to shear stress or to effects on soluble cue gradients[94]. In vitro and in vivo studies show that interstitial fluid flow promotes migration mediated by the C-X-C chemokine receptor type 4 (CXCR4) receptor and, to a lesser degree, by CD44–HA interactions[95–97]. The composition of interstitial fluid substantially varies by tumour region. Lack of dissolved oxygen (hypoxia) and low pH are characteristic of interstitial fluid in the tumour core, which perpetuates necrosis and drives tumour cells towards invasive and pro-angiogenic phenotypes[98]. The high interstitial fluid pressure (IFP) in solid tumours is a major barrier to chemotherapeutic delivery because it prevents the transport of small molecules into the tumour core[91]. Some therapeutic treatments cause a decrease in IFP, which could improve the therapeutic efficacy and reduce oedema. In particular, treatment with bevacizumab in orthotopic GBM models causes a reduction in IFP by ~73%, likely owing to a normalization of the vascularity[99] (BOX 1). The importance of interstitial fluid in GBM is well established; however, therapeutic interventions to target interstitial fluid are limited.

Tumour cells and stromal cells in the TME co-evolve during tumour progression. Immune and inflammatory cells, such as infiltrating monocytes and fibroblasts, endothelial cells and glioma-associated mesenchymal stem cells (MSCs), which are located throughout the tumour and in the intraparenchymal region, interact with tumour cells, driving disease progression (FIG. 1). Tumour cells also interact with other intraparenchymal stromal cells, such as astrocytes, pericytes, oligodendrocytes and neurons. A common and crucial function of these non-tumour cells is to secrete signals that modulate tumour cell survival, proliferation and migration. For example, MSCs secrete exosomes and soluble cytokines, such as interleukin-6 (IL-6), which interact with GSCs, increasing their proliferation and stemness[100,101]. Tumour-associated astrocytes (TAAs) release secreted factors that support tumour cell survival and proliferation, modulate the intratumoural immune response and promote invasion by activating tumour-derived matrix-remodelling enzymes, including MMPs and urokinase-type plasminogen activator (uPA)[102]. GBM cells also extensively interact with microglia and infiltrating tumour-associated macrophages (TAMs) to suppress an antitumour immune response[66,103,104]. Neurons promote proliferation of GBM cells through secretion of soluble factors such as neuroligin-3 (REF.[105]). Tumour cells also closely interact with vascular endothelial cells (FIG. 1c,e). For example, endothelial cells secrete IL-8 and GSCs upregulate IL-8 receptors, which stimulates migration, growth and stemness[106]. Tumour cells can further directly participate in vessel mimicry by aligning with

endothelial cells to form vascular walls or by trans-differentiating into endothelial cells[107,108]. Therefore, the incorporation of the stromal secretome in engineered TMEs is important, owing to its crucial role in regulating tumour cell behaviour, particularly in the context of immunotherapy.

Targeting the microenvironment

The TME substantially changes over time and in the different microregions, particularly during therapeutic treatment. Magnetic resonance imaging (MRI) scans of newly diagnosed patients typically reveal a contrast-enhancing, irregularly shaped GBM tumour border with pseudopalisades or regions of high cell density, surrounding a hypointense region of necrosis[109] (FIG. 1a,b). Necrotic cores are thought to arise once the tumour cell density exceeds a certain threshold at which the cells can no longer be supported by diffusion-based transport of nutrients, gases and metabolites from deteriorating or occluded vasculature. As cells migrate away from hypoxic regions, pseudopalisades form and recruit new vasculature[110] (FIG. 1b,c). As the tumour grows and invades, the adjacent tissue deteriorates (FIG. 1d,e). Neurodegeneration is caused not only by mechanical stresses[80] but also by aberrant levels of tumour-secreted soluble factors, such as the extracellular domain of CD44 (REF.[111]). Surgical resection of >98% of the gross tumour, including necrotic and pseudopalisading regions, increases overall patient survival[112]. Metabolic, fluorescent dyes can be employed during surgery to improve the identification of the tumour edge, although the clinical benefit is not yet clear[113]. Carmustine-releasing Gliadel wafers can be implanted following surgical resection and may especially benefit patients for whom gross resection is unfeasible; however, the efficacy and safety of this approach remain controversial[114,115]. Tumour-treating fields (alternating electric fields) that disrupt mitosis may also improve patient survival[116,117].

Glioblastoma stem cell niches. The resection of diffusely invading cells beyond the gross tumour edge poses risks of destroying functional tissue. Even if resection is performed beyond the tumour edge, there is no assurance that all tumour cells can be located and resected[5]. The clinical need for therapies targeting the remaining tumour cell population has motivated the investigation of how the TME promotes survival, invasion and proliferation of diffusely infiltrating tumour cells. GSCs are especially adept at invading healthy tissue and resisting chemotherapy and radiotherapy, which makes them a key candidate for targeted adjuvant therapies. GSCs reside within specific anatomic niches, which are specialized microenvironments that regulate GSC stemness, proliferation and apoptosis resistance, analogous to tissue stem cell niches[83,118–120]. Importantly, these niches shield GSCs from anticancer therapies by providing pro-survival cues and by anatomically blocking them from therapy exposure[121]. Four unique zones (subarachnoid, perineuronal, perivascular and perinecrotic) have, thus far, been identified that support GSC self-renewal and proliferation[120]. Each zone has a distinct TME composition with niche-specific transcriptional and epigenetic signatures[119,120].

The contributions of the perivascular niche to therapy resistance, infiltration spread and disease progression are perhaps best understood[83,118,122–124]. In the perivascular niche, GSCs and the TME engage in cooperative signalling, promoting neovascularization and GSC maintenance. The leaky vasculature provides access to nutrients, and the endothelium activates Notch-dependent pathways that promote GSC self-renewal and therapy resistance[125]. In turn, GSCs support neovascularization by secreting angiogenic factors such as VEGF[126]. Interestingly, endothelial-derived nitric oxide increases the tumour-initiating capacity of the platelet-derived growth factor receptor (PDGFR)-expressing subset of GSCs[127]. Matrix composition and mechanics of the perivascular niche also drive GSC tumourgenicity[83]. In particular, HA regulates GSC stemness by engaging the HA-specific cell surface receptors RHAMM[128] and CD44 and by activating the transcription of stemness modulators[129]. HA also activates the Toll-like receptor (TLR) 4–nuclear factor (NF)κB pathway to promote stemness; the expression of TLR4 receptors is upregulated during GSC differentiation along with HA synthesis, which increases NFκB activity and suppresses terminal GSC differentiation[130]. Furthermore, altered mechanotransduction caused by niche remodelling stimulates GSC tumourgenicity[131]. For example, a pro-tumourigenic glycocalyx–integrin feedforward loop, in which ECM stiffening induces a mesenchymal transition in GSCs, drives GBM progression correlated with poor prognosis[132–135]. In a brain-mimetic biomaterial platform for the 3D culturing of patient-derived GBM cells, the modulation of both the HA content and of the mechanical properties of the biomaterial are required to recreate the known resistance of GBM cells to the EGFR inhibitor erlotinib, highlighting that the TME can diminish therapeutic efficacy[136].

Although less understood, hypoxic GSC niches also substantially contribute to the maintenance of GSC populations[98,137,138]. Hypoxic niches arise when defective vessels are obstructed or collapse, which leads to a reduction in oxygenation[138]. Cells adapt to low oxygenation by activating hypoxia-inducible factors (HIFs)[98]. Activation of HIF-1α promotes GSC self-renewal and growth and causes pro-invasive protein expression through upregulation of CXCR4, which is a chemokine receptor related to increased migration[137]. Similarly, HIF-2α promotes the expression of Oct4, which is a stem cell marker strongly associated with stemness[139]. Interestingly, HIF-2α is specifically expressed by GSCs and, thus, may serve as a potential GSC-specific marker[139]. Hypoxia may even promote the reprogramming of non-stem GBM cells towards a GSC-like phenotype[139]. Therefore, TME niches play a multifaceted role in regulating GSCs, motivating their investigation in engineered TME models.

Microenvironmental changes. Radiotherapy increases overall patient survival by reducing tumour burden and by improving BBB permeability for chemotherapeutics; however, radiotherapy also triggers the remodelling of the TME, which increases the aggressiveness of tumours

at recurrence[140]. In response to radiation, TAMs infiltrate the tumour through the defective BBB and astrocytes adopt a reactive phenotype, which induces tissue inflammation[140]. Moreover, in contrast to bulk tumour cells, GSCs are particularly efficient at evading radiotherapy by activating DNA damage checkpoints to repair DNA damage[141]. The TME promotes tumour cell survival during radiation treatment; for example, in a co-culture of GSCs with astrocytes, signal transducer and activator of transcription 3 (STAT3), signalling is activated in GSCs in response to astrocyte-secreted factors, which increases GSC radiation resistance[142]. Radiation further temporarily induces senescence in GBM cells by triggering a 'senescence-associated secretory phenotype', which leads to upregulation of ECM expression, proteolytic enzymes and pro-inflammatory signalling molecules[140]. After exiting senescence, these cells and their microenvironments are primed for invasion and proliferation. GBM cells increase HA production in response to radiation by increasing the expression of HAS2, which correlates with increased invasion[41]. Senescence also occurs in stromal cells[140] and tumour cells can compensate for endothelial cell senescence by transdifferentiating into endothelial cells, enabling angiogenesis[143].

The chemotherapeutic temozolomide (TMZ) increases patient survival but can trigger TME remodelling that promotes a resistant, pro-invasive tumour phenotype. Treatment of cultured GBM cells with radiation and TMZ induces an increase in MMP-2 secretion and abundance of matrix-degrading invadopodia[144]. TMZ treatment also alters proteoglycan and GAG composition, with the combination of TMZ and dexamethasone resulting in deterioration of proteoglycan and GAG content[145]. Other agents promote TME remodelling that slows tumour progression. Microtubule inhibitors target cell division, but they can also reduce the invasive capacity of tumour cells by reducing MMP-2 expression[146]. Dexamethasone, which is a steroid traditionally applied for its ability to reduce oedema rather than for its chemotherapeutic properties, also activates fibronectin matrix assembly, resulting in increased cell–cell and cell–matrix adhesions that may slow invasion[51]. However, the role of dexamethasone and other steroids in tumour progression and their interactions with therapeutic interventions are largely unknown. The investigation of treatment-induced TME remodelling in engineered models could unravel these interactions to improve therapeutic strategies.

Table 2 | **Tumour microenvironment-targeted drugs in clinical trials**

Therapeutic agent	Target	Effect on tumour progression in preclinical models	Refs
Microglia and TAMs			
PLX3397	CSF1R inhibitor	↓Microglia, ↓tumour burden, ↓invasion	150
Cell receptor–ECM interactions			
Cilengitide	Pentapeptide that blocks activation of αvβ3 and αvβ5 integrins	↓Angiogenesis and tumour growth by blocking of integrins on vascular endothelial and tumour cells	167
Hypoxia			
AQ4N	Bioreductive prodrug targeting topoisomerase II in hypoxic cells	↓Hypoxic cells	163
Microvascular-related pathways			
Tivozanib	Pan-VEGFR tyrosine kinase inhibitor	↓Proliferation, ↓expression of VCAM-1-mediated and ICAM-1-mediated cell–cell adhesion, and ↓MMP-2-mediated invasion	155
Sunitinib	PDGFR and VEGFR inhibitor	↓Angiogenesis, ↓proliferation	158
Cediranib	Pan-VEGFR tyrosine kinase inhibitor	↓Angiogenesis, normalization of vasculature	156,157
AMG 386	Angiopoietin-1-neutralizing/angiopoietin-2-neutralizing peptibody	↓Vessel permeability, ↓angiogenesis	159,160

CSF1R, colony-stimulating factor 1 receptor; ECM, extracellular matrix; ICAM-1, intercellular adhesion molecule 1; MMP-2, matrix metalloproteinase 2; PDGFR, platelet-derived growth factor receptor; TAM, tumour-associated macrophage; VCAM-1, vascular cell adhesion molecule 1; VEGFR, vascular endothelial growth factor receptor.

Targeted therapeutic agents. Targeting therapeutics to the tumour and the TME offer promise to improve patient survival and quality of life[147,148]. Successful clinical treatment of chronic myeloid leukaemia and gastrointestinal stromal tumours with the small-molecule inhibitor imatinib mesylate (Gleevec) targeting mutated kinases demonstrated the potential of targeted therapies[147]. Targeted therapies have also been clinically successful in breast cancer treatment, particularly for the human epidermal growth factor receptor 2 (HER2)-amplified subset[148]. Unfortunately, most of the clinically tested GBM-targeted therapies have shown little efficacy thus far, such as erlotinib targeting the often overexpressed EGFR or PLX3397 targeting colony-stimulating factor 1 receptor (CSF1R) to modulate TAM activity[16,149,150]. Inhibitors targeting the hypervascularity of GBM tumours have come closest to realization and remain a promising strategy (TABLE 2). The anti-VEGFA therapeutic bevacizumab is currently the only drug approved by the US Food and Drug Administration (FDA) targeting the GBM TME[151–153]. Bevacizumab treatment initially causes a decrease in tumour volume and vascularity, but tumours ultimately adapt with revascularization and increased invasiveness[154]. A more potent pan-VEGF family inhibitor, tivozanib, reduces proliferation and invasion, and is currently undergoing clinical evaluation[155]. Similarly, inhibitors of VEGF receptor tyrosine kinases, such as cediranib and sunitinib, show promise in reducing angiogenesis and normalizing vascularization[156–158]. Other angiogenic targets are also under investigation; for example, the angiopoietin inhibitor AMG 386 reduces vascular permeability and angiogenesis[159,160]. The potential of antiangiogenic therapies motivates the investigation of vascular–tumour interactions in engineered TME models.

Several other TME features are also explored as targets (TABLE 2). Efforts to eradicate hypoxic cells within the TME have, overall, been positive in clinical trials in patients with advanced solid tumours[161–164]. Bioreductive prodrugs can be enzymatically reduced in hypoxic regions into cytotoxic products. AQ4N is a bioreductive

prodrug targeting topoisomerase II and it has shown promise as an adjuvant therapy in preclinical trials of several cancers, including GBM[164]. Importantly, AQ4N can cross the BBB and was well tolerated in all patients in a phase I study in GBM[163]. Cell–matrix interactions represent another key target for therapies[165–167]. Cilengitide is the first integrin inhibitor undergoing clinical testing and initially showed promise for modestly improving survival in both newly diagnosed and recurrent GBM with tolerable toxicity[167]. Cilengitide inhibits integrins αvβ3 and αvβ5, which are overexpressed on GBM cells and vascular endothelial cells. This inhibition disrupts angiogenesis and tumour–matrix interactions needed for migration. However, cilengitide was eventually shown to be ineffective in phase III clinical trials[168], which may be related to poor bioavailability; thus, cilengitide may warrant further investigation[169]. Careful consideration of how the TME influences tumour mechanics and transport can be leveraged to improve drug-delivery methods[165]. For example, convection-enhanced delivery involves catheter insertion directly into the tumour core to continuously deliver a chemotherapy, avoiding perfusion across the BBB and counteracting resistance from increased interstitial pressure[170]. Moreover, a poliovirus-based immunotherapy designed to activate oncolytic T cells has shown promise in improving GBM patient survival and may be combined with molecularly targeted therapeutic stragies[171,172].

Engineering microenvironment models

Experimental models for GBMs range in complexity from 2D cultures on glass or plastic to orthotopic xenografts and genetically engineered mouse models[29]. Traditional 2D models have proven invaluable for investigating some molecular mechanisms governing GBM progression, such as early studies elucidating how MMPs and soluble factors contribute to tumour initiation, invasion and propagation[173]. However, 2D models lack the ECM stiffness and composition, topographical guidance cues and dimensionality of human tissue needed to fully investigate the role of the TME. Orthotopic xenografts of patient-derived GBM cell lines in immunodeficient murine models are commonly used to fully recapitulate the in vivo TME. Orthotopic xenograft models better mimic tumour heterogeneity than in vitro models, with different levels of tumour heterogeneity, depending on the model[174,175]. However, orthotopic xenograft models lack a normal immune response, which is a key parameter in regulating tumour progression and full retention of tumour heterogeneity[28,176]. Furthermore, animal models are more expensive and less scalable than in vitro models, and are often impractical for detailed mechanistic dissection of human pathobiology[177]. The GBM TME substantially affects tumour progression and, thus, engineered TME models offer a valid alternative as experimental GBM models with the potential to overcome the limitations related to animal models[178]. Specific parameters (ECM composition, mechanics, topography and stromal cells) can be incorporated into engineered models to recreate the GBM TME for more precise hypothesis testing (TABLE 3).

2D matrix models. A simple approach to incorporating TME components into engineered models is to fabricate 2D substrates featuring ECM ligands and mechanical properties normally present in brain matrix. These modified 2D substrates can be used to explore how matrix mechanics and ECM components affect cell morphology, proliferation and migration (FIG. 2a). The mechanical properties of synthetic substrates, such as polyacrylamide (PA)[72,74,75,78,179] and silicone rubber[73], can be well controlled in a physiologically relevant range and coated or conjugated with cell-adhesive matrix proteins, such as laminin or fibronectin. Natural or semi-synthetic polymer matrices, such as collagen[180,181] and HA[77,182,183], typically contain some adhesive ECM cues, but they can also be further modified with ligands. HA gels are particularly advantageous for recapitulating the HA richness of brain ECM. A diverse array of chemistries can be applied in HA gels, such as the addition of methacrylate or thiol groups, to facilitate crosslinking and modification with peptides[183–185]. Synthetic and natural 2D substrates have been applied to demonstrate that GBM cells are mechanoresponsive and that the mechanical response varies between patients and between subpopulations of cells[74,75]. For example, our laboratory has employed 2D HA hydrogels to show that CD44 can transduce mechanical signals from HA to regulate GBM adhesion and invasion[77].

3D matrix models. 2D platforms can be rapidly fabricated, are parallelizable and amenable to imaging and culture manipulations; however, owing to their 2D nature, they cannot fully capture brain architecture. By contrast, 3D matrices offer the possibility to incorporate soluble cue gradients, such as an oxygen gradient, and confinement of invading cells, which alters cell morphology and requires the cells to degrade or squeeze through the matrix — as is the case in an in vivo TME. Interestingly, dimensionality alone can profoundly affect cell responses to chemotherapeutics, independent of matrix stiffness or composition[181]. Materials used for 2D substrates, such as collagen[181,186–190] and HA[123,183], can also be employed as 3D scaffolds. However, materials such as PA or polycaprolactone (PCL) requiring harsh solvents or crosslinking reagents during gelation cannot be easily seeded with cells unless they are made highly porous, such that cells can be incorporated into the matrix after gelation. Matrigel, which is a reconstituted basement membrane harvested from mouse sarcoma, is commonly used as 3D matrix because of its rapid, temperature-based gelation, abundance of adhesive sites and compositional complexity[118,191,192]. Collagen and Matrigel are simple to use relative to materials requiring complex synthesis, compatible with 3D cell encapsulation and contain various adhesive sites; however, the collagen-rich composition of both matrices and the fibrous architecture of collagen do not resemble the HA-rich, nanoporous brain matrix. Additionally, Matrigel composition is poorly defined chemically and exhibits batch-to-batch variability. Alternatively, synthetic polyethylene glycol (PEG) gels can be decorated with adhesive peptides and crosslinked with cleavable linkers, enabling precise control over matrix mechanics

and composition for GBM modelling. Incorporation of degradability into 3D PEG matrices is not required for GBM cell viability and colony expansion but is essential for mesenchymal-like cell spreading[193]. 3D scaffolds, including electrospun polystyrene (PS) coated with laminin[194], porous PCL scaffolds with incorporated HA[195], poly(N-isopropylacrylamide-co-Jeffamine M-1000 acrylamide) (PNJ) copolymer scaffolds[196] and electrolyte complexes of alginate and chitosan[197], have been applied to demonstrate that dimensionality and matrix cues synergistically support maintenance of GSC stemness. More complex matrices can be fabricated by

Table 3 | **Engineered glioblastoma models**

Model	Key findings	Refs
2D matrix models		
PA	Spreading, migration and proliferation increases with matrix stiffness, depending on tumour cell subpopulation and patient	72,74,75, 78,179
Silicone rubber	Spreading increases with elastic modulus	73
Collagen	Matrix biophysical properties affect phenotype	180,181
HA	CD44 is mechanosensitive; elastic modulus affects microRNA expression	77,182,183
3D matrix models		
Collagen	Dimensionality determines drug resistance; porosity and density affect invasion speed	181,186, 189,190
Collagen–agarose	Cell spreading and motility in collagen requires local matrix stiffening	187,188
HA	Cell invasion through HA mimics invasion in the brain and is slow relative to invasion in highly porous matrices	123,183
Matrigel	Stromal cells in 3D matrix affect GBM phenotype	118,191,192
PEG	MMP degradability enhances cell spreading	193
PNJ	Scaffolds increase stemness of GSCs	196
PCL–HA	HA maintains stemness of GSCs	195
Alginate–chitosan	Scaffolds increase stemness marker expression	197
HA–collagen	HA upregulates invasion	207
HA–gelatin	HA upregulates matrix remodelling	45,208
HA–PEG	Matrix elastic modulus affects ECM deposition	209
Brain-derived ECM	Cells exhibit brain-like invasion in matrix	198,199
Models of heterogeneity		
Elastic modulus patterning	Higher modulus increases cell spreading in 2D and 3D	215,217
Orthogonal parameter patterning	Composition and stiffness have non-linear effects on phenotype	182,216
Soluble cue gradient	Reduced nutrient and oxygen transport increases secretion of angiogenic factors	218
Topographical models		
ECM interface	Interface properties drive invasive morphology	219,220
Open channels	Stiffness and pore size have combined effect on invasion	179
Electrospun fibres	Linear topographic cues drive rapid invasion	194,221–226
Encapsulated fibres or channels	Cells transition to rapid invasion when encountering linear topographic cues in 3D matrix	123,207
Interstitial fluid models		
Flow in Boyden chamber	Interstitial flow drives CXCR4-dependent invasion	95–97
Multiparameter microfluidic and bioprinted systems		
Pseudopalisade model	Vaso-occlusion drives migration and pseudopalisade formation	228
PVN models	Stromal-cell crosstalk affects invasive phenotype	199,229–231
Mini-brain with macrophages	GBM cells recruit and influence macrophage polarization	238
Organoid		
Tumour organoid culture	Tumour organoids maintain heterogeneity and hypoxic gradient	239
Stem-cell-derived tissue	Engineered neural tissue supports brain-like GBM invasion	241

CXCR4, C-X-C chemokine receptor type 4; ECM, extracellular matrix; GBM, glioblastoma; GSC, glioblastoma stem cell; HA, hyaluronic acid; MMP, matrix metalloproteinase; PA, polyacrylamide; PCL, polycaprolactone; PEG, polyethylene glycol; PNJ, poly(N-isopropylacrylamide-co-Jeffamine M-1000 acrylamide); PVN, perivascular niche.

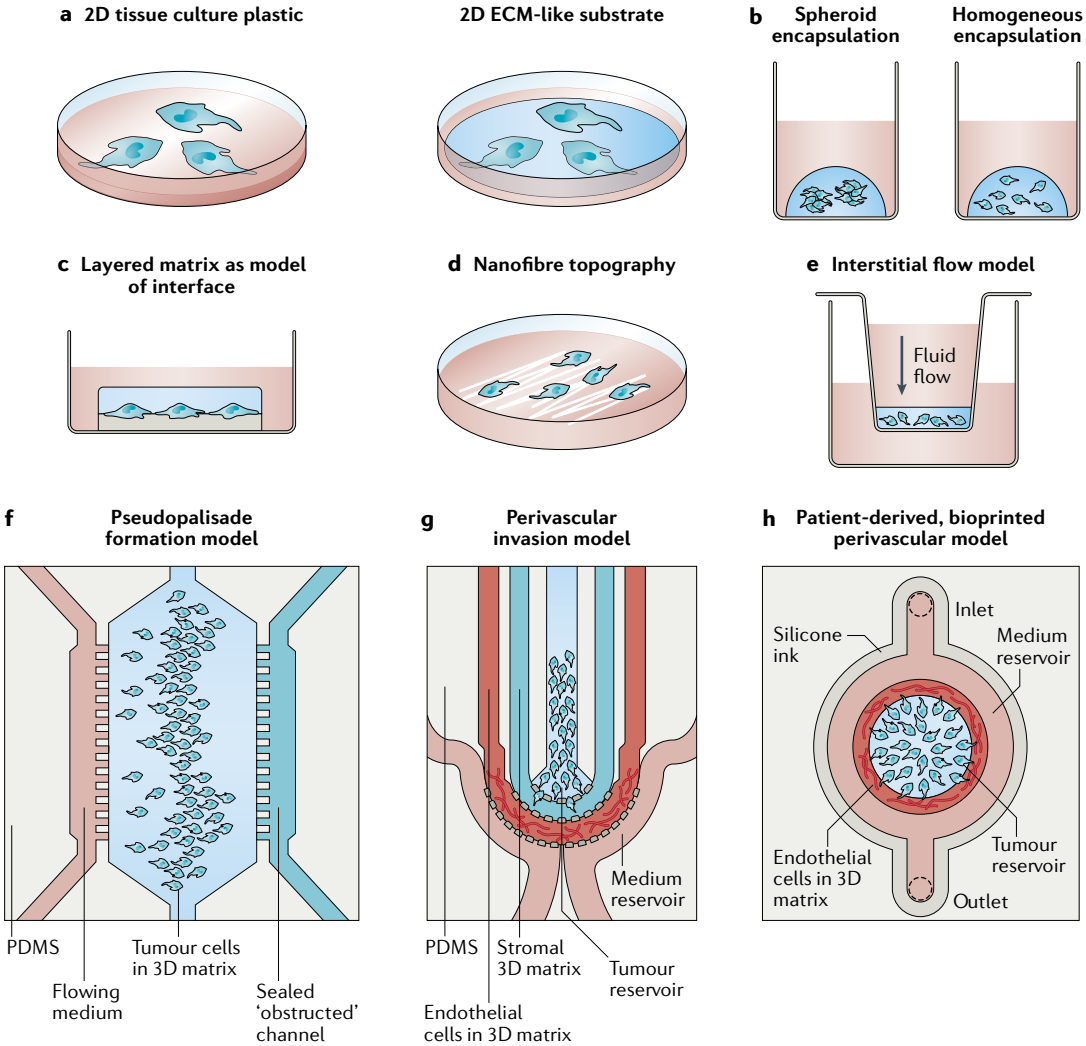

Fig. 2 | **Engineered glioblastoma models. a** | 2D models often include a matrix layer with tunable mechanical properties and composition. **b** | In 3D matrices, cells can be encapsulated as spheroids or as single cells. **c** | Cells can be cultured between extracellular matrix (ECM) layers of distinct composition and mechanics to model cell migration at the interface of the vascular basement membrane and the intraparenchymal matrix. **d** | Nanofibres with ECM coatings are often used to mimic linear, white-matter tracts. **e** | Media height in a Boyden chamber can be used to generate interstitial flow through matrix-encapsulated cells. **f** | A microfluidic device with an open (nutrient-rich) and closed (occluded) channel surrounding matrix-encapsulated cells can be used to test how pseudopalisades form. **g** | A microfluidic model of the perivascular niche containing a glioblastoma stem-cell-rich tumour reservoir, an intraparenchymal region with stromal matrix and a region of matrix-encapsulated endothelial networks can be used to investigate the role of the perivascular niche in glioblastoma stem-cell tumourgenicity. **h** | A bioprinted microfluidic model with a matrix-encapsulated endothelial network arranged concentrically around patient-derived tumour cells can be applied for the development of patient-specific engineered tumour microenvironments. PDMS, polydimethylsiloxane. Panel **f** adapted from REF.[228], Ayuso, J. M. et al. Glioblastoma on a microfluidic chip: generating pseudopalisades and enhancing aggressiveness through blood vessel obstruction events, *Neuro. Oncol.* (2017) **19**, 230, by permission of Oxford University Press, Society of NeuroOncology. Panel **g** is adapted with permission from REF.[229], Elsevier. Panel **h** is adapted from REF.[199], Springer Nature Limited.

combining decellularized porcine or patient-derived brain matrix with low amounts of collagen, which better mimics the compositional complexity of the brain[198,199]. However, these matrices are limited by sample size and require processing steps that destroy the native protein structure.

Cells can be embedded into 3D hydrogels as tumourspheres or as homogeneously dispersed single cells (FIG. 2b). Spheroids recapitulate the soluble cue gradients present in tumours, and spheroids with large diameters (>500 μm) exhibit a hypoxic and sometimes necrotic core[200]. GSCs cultured as tumourspheres in serum-free medium better maintain stemness and heterogeneity than GSCs cultured as single cells in serum-containing medium, and they can be directly encapsulated into matrices[201]. Adherent cells can be grown as tumourspheres using a hanging drop culture[202] or microwells[203] to aggregate cells into spheroids. Homogeneous dispersion of single cells, which are typically encapsulated during matrix gelation, enables evaluation

of single-cell morphology, proliferation and colony growth[193,204]. In matrices with large pores, liquid cell suspensions can be dropped onto dehydrated, hydrophilic scaffolds; the cells are then drawn into the bulk 3D matrix after rapid absorption. This approach allows the incorporation of cells into matrices with harsh fabrication chemistries, such as electrospun PS or porous PCL[194,195]. Stromal cells can also be integrated into 3D matrices together with tumour cells but with limited possibilities to control their spatial organization. Stromal cells strongly influence GBM cell behaviour; for example, GBM cells cultured with astrocytes and endothelial precursors in 3D HA–collagen matrices exhibit increased migration speed and resistance to STAT3 inhibition as compared to GBM cell culture alone[205].

HA-containing matrices can be fabricated by directly crosslinking the HA backbone[136,183], by complexing HA with polycations such as chitosan[206] or by mixing or conjugating HA into hydrogel networks with collagen[207], gelatin[45,208] or PEG[209]. The nanoporosity (~100–200 nm mesh size) of crosslinked HA gels impedes cell squeezing, necessitates more cell-mediated matrix degradation and leads to slower invasion than matrices with large pores, such as collagen[183,184,190]. HA can also be mechanically incorporated into gelatin matrices with variable elastic moduli and growth factor concentrations. The specific combinations of modulus and growth factor differentially affect proliferation and invasion[210]. Using high-molecular-weight HA, as compared with low-molecular-weight HA, in gelatin matrices leads to an increase in HA production by GBM cells and a decrease in cellular invasion, without changes in HA synthase or hyaluronidase protein expression[45]. The presence of HA in 3D models further induces resistance to the EGFR inhibitor erlotinib, mediated by CD44 (REF.[211]), as well as altered RHAMM, HAS1 and HAS2 gene expression[124]. The effect of HA on resistance to erlotinib depends on the mutant status of EGFR, which can vary between patient-derived lines[212]. Thus, the incorporation of HA into engineered TME models has revealed key mechanisms by which HA drives GBM progression.

Engineering gradients. Mechanical and biochemical ECM cues in the brain are often spatially organized, for example, as gradients or localized hotspots. Spatial organization can be recreated by 2D substrate patterning using photolithographic and microfabrication techniques in combination with aqueous photochemistries[213,214]. For example, polydimethylsiloxane (PDMS) substrates can be patterned with different stiffnesses by generating stiff posts of defined shapes and sizes, which can be attached to the underside of a thin PDMS membrane. Fibroblasts and myoblasts cultured directly opposite the pillars on the flat upper side of the membrane experience the highest stiffness and show a haptotactic response by migrating towards or along stiff features[215]. Patterning substrates with ECM or mechanical gradients can be used for high-throughput parameter space testing or to examine cell responses to brain-like haptotactic cues. For example, orthogonal patterning of a fibronectin and elastic modulus gradient on an HA hydrogel revealed that GBM cells spread and express oncogenic microRNA in a non-linear manner across the range of the gel[182]. Patterning of 3D substrates is limited by the available patterning method. For example, microfluidic mixing of HA and gelatin precursor solutions with different concentrations results in 3D gelatin–HA gels with gradients of crosslinking density, in HA content and, subsequently, in cell density[216]. Interestingly, cells in these gels showed a biphasic MMP9 expression profile with increasing HA concentration. 3D gels can also be attached to a glass surface, resulting in a non-linear stiffness gradient along the *z*-axis. Cells encapsulated less than 25 µm from the glass surface spread more and migrate faster than cells located >500 µm from the glass surface independent of matrix density, demonstrating that distance from the glass substrate to the cells within the gel could be used to investigate mechanical effects on GBM[217]. Soluble cue gradients, including oxygen gradients and hypoxia, arise naturally in bulk 3D gels submerged in medium as a function of gel thickness. Cells seeded in 2-mm-thick gelatin hydrogels are exposed to lower rates of nutrient transport and show a pro-angiogenic phenotype with increased VEGF and HIF-1 expression, as compared with cells cultured in 1-mm-thick gelatin hydrogels[218]. Therefore, these TME models can be applied to elucidate the mechanisms by which spatial variation in mechanics, ECM composition and soluble cues influence tumour progression.

Engineering interfaces and topography. Semi-3D materials, often referred to as 2.5D materials, are characterized by a 3D topology arising from multiple 2D topologies. 2.5D systems combine the practicality of fabricating 2D features or patterns with the possibility to incorporate 3D-like constraints. In certain cases, these systems more faithfully recapitulate tissue architecture than 'true' 3D matrices. For example, the interface between the vascular basement membrane and the intraparenchymal ECM has been modelled by consecutively layering materials that are representative of the two regions (FIG. 2c). The bottom layer fabricated from Matrigel is analogous to the vascular membrane and the top layer of viscous, soluble HA is analogous to the parnechyma[219]. GBM spheroids seeded at the interface of the two layers show rapid, collective cell migration along the interface when the top layer includes highly viscous HA or viscous methylcellulose, as compared with little invasion when the top layer does not include viscous HA or methylcellulose. Thus, the presence of an interface between a matrix layer and highly viscous solution is sufficient to guide cell invasion along vascular membranes. The migration speed of cells seeded between fibronectin-coated PA and crosslinked HA or crosslinked HA conjugated with the integrin-binding peptide RGD depends on the degree of ligand–receptor interactions between the cells and the interface, with more interactions slowing invasive migration speed[220]. Semi-3D substrates resembling the brain intraparenchymal region can also be fabricated by layering ECM-producing astrocytes onto plastic to form a parenchyma-like substrate[219]. GBM invasion speed on astrocyte layers inversely correlates with the culture time of astrocytes, which may be a result of ECM accumulation or changes in astrocyte phenotype.

GBM cells rapidly invade along anatomical tracks, specifically in the perivascular space or on myelinated axons[18]. Engineering models of anatomical tracks typically include a linear, topographical feature fabricated on a 2D surface or encapsulated in a 3D matrix. Confinement imposed by microchannels can recapitulate the linear migration and squeezing that cells exhibit when invading tight spaces along anatomical tracks. PA microchannels can be employed to independently modulate pore size and modulus, and have been used in our laboratory to show that matrix modulus and confinement synergize to promote rapid invasion[179]. Alternatively, nanofibres can be applied to study the effects of aligned topographical cues resembling the orientation of white-matter tracts. Interestingly, aligned fibres strongly promote rapid, linear migration[221–226] (FIG. 2d). To decouple the surface chemistry from the fibre mechanics, electrospun fibres with a 'core' material surrounded by a 'shell' of a different material were fabricated. The core material determined the modulus, while the shell material determined the surface chemistry. Varying material combinations for the shell and core were employed to demonstrate that GBM cell migration and morphology are sensitive to both nanofibre modulus and ECM coating[225]. The basement membrane composition and topographical features can be recreated within a 3D matrix by coating microfibres with Matrigel and embedding them in 3D matrices. Invading cells that encounter microfibres switch to an invasive mode and rapidly migrate along the fibres[207]. ECM-coated nanofibres also modulate GSC stemness, with laminin-isoform-specific effects[194]. Thus, topographical cues strongly drive invasion, proliferation and resistance, which can be enhanced by other TME signals, such as ECM composition and increasing stiffness.

Interstitial fluid in engineered models. Little is known about how interstitial fluid flow and pressure direct GBM invasion. Interstitial fluid flow can be modelled by seeding hydrogel-encapsulated cells in a Boyden chamber. The top chamber is then filled with excess medium, which creates pressure-driven fluid flow through the membrane pores in parallel to cell migration (FIG. 2e). Using such a model, it could be demonstrated that the interstitial fluid flow activates CXCR4-dependent polarized cell migration in multiple GBM cell lines, including GSCs[95,96]. This CXCR4-dependent invasion was confirmed in a mouse model, in which convection-enhanced therapy was applied to control interstitial flow[97], highlighting the clinical importance of fluid flow for tumour progression and convection-enhanced therapy[97,170].

Microfluidic models with multiple cues. Adding more complexity to TME models improves physiological relevance but, typically, increases the required labour and sacrifices throughput[29]. Microfluidic models can be made complex enough to facilitate construction of TME models with fluid flow, 3D ECM, spatial organization and stromal cell co-culture in a single platform, while allowing imaging, control of parameters and high-throughput screening[227], as well as achieving cost-effectiveness, compared with in vivo models. For example, a device with three parallel, adjacent channels has been developed to test the hypothesis that pseudopalisades form as migrating cells accumulate after a vaso-occlusive event[228] (FIG. 2f) . The outside channels contain flowing medium and the centre channel contains a 3D matrix with homogeneously encapsulated cells. Vaso-occlusion can be mimicked by stopping the flow through one channel, which results in a hypoxic gradient. GBM tumour cells migrate away from the occluded channel and form pseudopalisades, supporting the mechanistic hypothesis.

The versatility of microfluidic devices also allows the reconstruction of TME niches. In particular, perivascular niche models can be constructed using parallel, interconnected channels to spatially organize niche layers. GSCs incorporated into such a microfluidic perivascular niche model featuring endothelial cells and the spatial organization of a GBM tumour exhibit morphologies, stemness markers and CXCR4-dependent invasion similar to those observed in vivo[229] (FIG. 2g) . Similarly, in a three-channel device with a tumour reservoir separated by a collagen matrix from an endothelialized, vascular-like reservoir, GSCs are known to precede their differentiated counterparts in invasion. Moreover, GBM pro-invasive genes, including integrins α2 and β3, are upregulated in the presence of endothelial cells[230]. Vascular homing can be studied using a microfluidic device, in which GSCs are encapsulated in a 3D microvascular network[231]. GSCs derived from the subtype of GBM tumours with high PDGFRA expression are particularly prone to vascular homing.

Microfluidic devices have also been developed for preclinical screening. Numerous wells can be included in a single device, seeded with tumourspheres and exposed to orthogonal gradients of chemotherapeutics and nutrients. These devices can serve as platforms for the optimization of drug efficacy and to predict therapeutic resistance[232–234]. However, how these results would translate to decisions for patient care remains unclear, given the difficulty in validating in vitro results with patient outcomes. The efficacy and toxicity of chemotherapeutics are significantly influenced by multiple organ system functions, particularly by the liver metabolism. Intestine and liver models can be added to a GBM model in a microfluidic device to allow chemotherapeutic screening, while considering pro-drug absorption by an intestine-like lumen, as well as metabolism by liver cells[235].

Bioprinting. Bioprinting, or 3D printing of biomatrices and/or cells, can be applied to organize and fabricate 3D matrices and microfluidic models[236,237]. For example, patient-specific GBM models can be bioprinted using concentric rings of endothelial and patient-derived tumour cells encapsulated in a porcine-brain-derived matrix[199] (FIG. 2h). Key tumour features, such as the hypoxia-induced necrotic core surrounded by pseudopalisades, were observed within the model. Importantly, printed tumours recapitulate clinically observed patterns of tumour resistance to standard therapeutic treatments. The printing of patient-specific tumour models is limited by the sample size of the resected tumour; however,

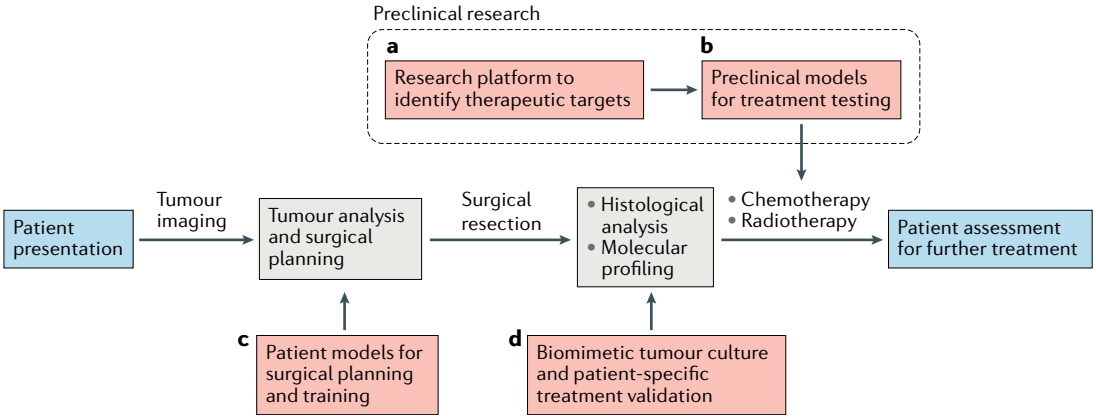

Fig. 3 | **Glioblastoma microenvironment models in the preclinical and clinical pipeline.** The red boxes indicate stages at which engineered models are or could be used. **a** | Engineered tumour microenvironments (TMEs) have been widely employed as research platforms to investigate the TME, and they can be used to identify therapeutic targets. **b** | With refinement, these platforms can serve as a basis for precision medicine using patient-specific cells and/or matrices. **c** | Images of tumours from patients can be used to generate mechanically matched, patient-specific models of the tumour and brain anatomy for surgical planning and training. **d** | After surgical resection, engineered TMEs can aid in maintaining heterogeneity during culture for patient-specific treatment validation. The cells can be selected by molecular profiling and histological analysis.

these results demonstrate the feasibility of incorporating a brain-derived matrix into printable bioinks in combination with patient-derived cell lines to test therapeutic responses. Similarly, bioprinted 'mini-brains' comprising a tumour-like, cell-dense region surrounded by a brain-shaped, macrophage-laden gel mimic the spatial organization of TAMs. The GBM cells in this model recruit macrophages and influence macrophage polarization; in turn, macrophages induce GBM invasion[238].

Organoid models of growth and invasion. Instead of recapitulating the complex brain matrix by controlled fabrication, cells can also be seeded into a matrix and stimulated to spontaneously develop into an organoid. To generate GSC organoids, patient tumour samples can be seeded directly into Matrigel suspended in medium. The suspended tumour cells grow into 'tumours' with diameters of 5–10 mm over 5–6 months[239]. In contrast to cell-isolation methods, in which the matrix is degraded and cells are disassociated, this method better preserves patient cell–matrix interactions and tumour heterogeneity, including the proportion of GSCs relative to differentiated cells found in the original patient tumour. During organoid growth, a GSC-rich hypoxic niche is formed at the centre of the organoid, which is surrounded by more rapidly dividing cells. Compared with cells cultured in spheroids, cells in organoids better mimic patient tumour phenotype and heterogeneity in orthotopic xenograft models, as well as therapeutic resistance in vitro. Similarly, cerebral organoids with organized, differentiated brain features have been developed for other disease models[240]. These approaches could also be combined to study GBMs. For example, in GSCs seeded in engineered human nervous tissue generated from pluripotent stem cells, the expression of more than 100 genes was upregulated by interactions of GBM cells with stromal cells, many of which relate to ECM remodelling[241]. Therefore, organoid models and engineered tissue can be applied to capture the complexity of tumour TMEs; however, their fabrication is time-intensive and they are difficult to reproduce. The benefits of complexity often do not outweigh the costs.

Opportunities for engineered models

Engineered GBM TME models have already provided a wealth of information about the function of the TME in GBM progression, including context-dependent mechanisms of GBM invasion and therapeutic resistance. With improved accuracy and (patho)physiological relevance, GBM TME models will play an important role in the preclinical and clinical pipeline (FIG. 3); for example, platforms incorporating patient-specific tumour samples may eventually aid in predicting therapeutic response and for the tailoring of treatments[228,232,239,242]. Drug responses are currently just as or more robustly predicted by molecular subtype, DNA methylation status and patient age than by in vitro testing. Furthermore, the limited treatment options in GBM arguably do not yet necessitate complex optimization strategies[1,243,244]. However, validated and reliable engineered models could greatly improve preclinical drug testing. Established mouse models for in vivo screening have already been incorporated as secondary endpoints in GBM clinical trials[245]; however, the time required for model development hinders timely translation into personalized therapies. Engineered TME models would allow therapy screening at shorter timescales. Furthermore, the development of microfluidic models of drug permeability across the BBB could be very valuable for evaluating drug delivery to the central nervous system[246]. Such models are already being developed, but require additional validation and standardization[247].

The translation of patient-specific anatomy to engineered models is also becoming achievable, owing to advances in 3D printing technologies[236]. Full-scale brain models can be generated from patient MRI scans and

have proven to be useful in pre-surgical planning, teaching and training[248]. For example, gelatin-based brain models have realistic mechanical properties and can be used for practicing gross resection without damaging intact tissue[249]. Further inclusion of a 3D-printed skull enables surgeons to practice cutting the skull and accessing the tumour site without unnecessarily damaging tissue[250]. Printing of patient-specific anatomical features combined with patient-derived cells and matrix may better recapitulate the gross tumour, facilitating at-scale studies of the TME. Such models could be useful for studying the influence of interstitial fluid on therapeutic delivery, for example, on drug release from Gliadel wafers or convection-enhanced delivery[114,170].

Machine-learning strategies can also be applied to GBM research. For example, algorithms can be used to extract functionally predictive information about the TME from MRI images. In particular, machine-learning-based parameterization of contrast enhancement in MRI images correlates with gene expression of distinct biological processes, such hypoxia, starvation, matrix remodelling and endothelial permeability[251]. Furthermore, image features can be correlated with tumour subtype and patient survival[252,253]. Patient-specific MRI data can then be combined with other patient characteristics, such as age and Karnofsky Performance Score, to improve diagnosis before surgical resection is performed[254]. Machine learning has also been explored to improve tumour segmentation[255]. This is particularly important for surgical planning but could also be applied for early diagnosis and therapy selection. The information derived from machine-learning algorithms could be combined with other TME modelling technologies to improve their accuracy.

Perspective and conclusions

The TME has demonstrated potential as a therapeutic target for GBM treatment, owing to its impact on tumour progression. Engineered microenvironments allow the investigation of cell responses in the context of the TME and, thus, facilitate rapid hypothesis testing and screening. However, challenges remain. In particular, the minimal model components necessary to accurately recapitulate in vivo mechanisms need to be determined and the accuracy of models needs to be validated. It remains unclear which of the numerous ECM formulations used in engineered models meet these minimal requirements. A reductionist approach in developing TME models is useful to mimic in vivo GBM cell behaviour while avoiding unnecessary costs and complexity. Validation ensures that in vitro discoveries generate useful predictions of clinical relevance. Validation strategies have not yet been fully standardized but generally fall into two categories. First, it has to be demonstrated that the physical parameters of the model, such as composition and mechanics, closely match those of brain, to make the model predictive of in vivo behaviour. Second, as a measure of model accuracy, cell phenotypes, such as migration, morphology, relative gene expression and chemosensitivity, should be similar to the in vivo phenotype. Ideally, it should further be verified that tumour progression in engineered models is driven by similar biochemical mechanisms as in vivo (for example, signalling pathways governing drug resistance), although this is currently rarely done. An iterative design cycle could be created, in which TME models are systematically tested, and the mechanistic and phenotypic predictions are checked against the in vivo response to refine the model and improve its predictive power.

Practical challenges that limit customizability and complexity include limited throughput and the need for composite fabrication techniques. Co-culture of GBM cells and stromal cells poses particular challenges, such as medium incompatibility, unmatched proliferation rates and long-term viability of primary stromal cells. Similarly, the inclusion of patient-derived cells or matrix in engineered models faces several challenges. Tumour matrix is difficult to obtain in large quantities and the acclimation of tumour cells to cell culture can alter their phenotype. However, these challenges can certainly be addressed in the future and engineered models offer the opportunity to rapidly and precisely dissect mechanisms of GBM progression, accelerate clinical testing and provide a platform for precision medicine.

Published online 16 August 2019

1. Ostrom, Q. T. et al. CBTRUS statistical report: primary brain and other central nervous system tumors diagnosed in the united states in 2011–2015. *Neuro. Oncol.* **20**, iv1–iv86 (2018).
2. Koshy, M. et al. Improved survival time trends for glioblastoma using the SEER 17 population-based registries. *J. Neurooncol.* **107**, 207–212 (2012).
3. Stupp, R. et al. Effects of radiotherapy with concomitant and adjuvant temozolomide versus radiotherapy alone on survival in glioblastoma in a randomised phase III study: 5-year analysis of the EORTC-NCIC trial. *Lancet Oncol.* **10**, 459–466 (2009).
4. Watanabe, M., Tanaka, R. & Takeda, N. Magnetic resonance imaging and histopathology of cerebral gliomas. *Neuroradiology* **34**, 463–469 (1992).
5. Young, R. M., Jamshidi, A., Davis, G. & Sherman, J. H. Current trends in the surgical management and treatment of adult glioblastoma. *Ann. Transl. Med.* **3**, 121 (2015).
6. Sherriff, J. et al. Patterns of relapse in glioblastoma multiforme following concomitant chemoradiotherapy with temozolomide. *Br. J. Radiol.* **86**, 20120414 (2013).
7. Eyler, C. E. & Rich, J. N. Survival of the fittest: cancer stem cells in therapeutic resistance and angiogenesis. *J. Clin. Oncol.* **26**, 2839–2845 (2008).
8. Franceschi, E. et al. Treatment options for recurrent glioblastoma: pitfalls and future trends. *Expert Rev. Anticancer. Ther.* **9**, 613–619 (2009).
9. Quail, D. F. & Joyce, J. A. The microenvironmental landscape of brain tumors. *Cancer Cell* **31**, 326–341 (2017).
10. Levental, K. R. et al. Matrix crosslinking forces tumor progression by enhancing integrin signaling. *Cell* **139**, 891–906 (2009).
11. Nakasone, E. S. et al. Imaging tumor–stroma interactions during chemotherapy reveals contributions of the microenvironment to resistance. *Cancer Cell* **21**, 488–503 (2012).
12. Ghajar, C. M. et al. The perivascular niche regulates breast tumour dormancy. *Nat. Cell Biol.* **15**, 807–817 (2013).
13. Provenzano, P. P., Inman, D. R., Eliceiri, K. W. & Keely, P. J. Matrix density-induced mechanoregulation of breast cell phenotype, signaling and gene expression through a FAK–ERK linkage. *Oncogene* **28**, 4326–4343 (2009).
14. Elahi-Gedwillo, K. Y., Carlson, M., Zettervall, J. & Provenzano, P. P. Antifibrotic therapy disrupts stromal barriers and modulates the immune landscape in pancreatic ductal adenocarcinoma. *Cancer Res.* **79**, 372–386 (2019).
15. Provenzano, P. P. et al. Enzymatic targeting of the stroma ablates physical barriers to treatment of pancreatic ductal adenocarcinoma. *Cancer Cell* **21**, 418–429 (2012).
16. De Vleeschouwer, S. & Bergers, G. in *Glioblastoma* Ch. 16 (ed De Vleeschouwer, S.) (Codon Publications, 2017).
17. Jain, A. et al. Guiding intracortical brain tumour cells to an extracortical cytotoxic hydrogel using aligned polymeric nanofibres. *Nat. Mater.* **13**, 308–316 (2014).
18. Gritsenko, P. G., Ilina, O. & Friedl, P. Interstitial guidance of cancer invasion. *J. Pathol.* **226**, 185–199 (2012).
19. Bellail, A. C., Hunter, S. B., Brat, D. J., Tan, C. & Van Meir, E. G. Microregional extracellular matrix heterogeneity in brain modulates glioma cell invasion. *Int. J. Biochem. Cell Biol.* **36**, 1046–1069 (2004).
20. van Tellingen, O. et al. Overcoming the blood–brain tumor barrier for effective glioblastoma treatment. *Drug Resist. Updat.* **19**, 1–12 (2015).
21. de Vries, N. A., Beijnen, J. H., Boogerd, W. & van Tellingen, O. Blood–brain barrier and chemotherapeutic treatment of brain tumors. *Expert Rev. Neurother.* **6**, 1199–1209 (2006).

22. Nimsky, C. et al. Preoperative and intraoperative diffusion tensor imaging-based fiber tracking in glioma surgery. *Neurosurg.* **56**, 130–138 (2005).
23. Giese, A. & Westphal, M. Glioma invasion in the central nervous system. *Neurosurg.* **39**, 235–252 (1996).
24. Miller, K., Chinzei, K., Orssengo, G. & Bednarz, P. Mechanical properties of brain tissue in-vivo: experiment and computer simulation. *J. Biomech.* **33**, 1369–1376 (2000).
25. Budday, S. et al. Mechanical properties of gray and white matter brain tissue by indentation. *J. Mech. Behav. Biomed. Mater.* **46**, 318–330 (2015).
26. Bernstein, J. J. & Woodard, C. A. Glioblastoma cells do not intravasate into blood vessels. *Neurosurg.* **36**, 124–132 (1995).
27. Nakod, P. S., Kim, Y. & Rao, S. S. Biomimetic models to examine microenvironmental regulation of glioblastoma stem cells. *Cancer Lett.* **429**, 41–53 (2018).
28. Lenting, K., Verhaak, R., ter Laan, M., Wesseling, P. & Leenders, W. Glioma: experimental models and reality. *Acta Neuropathol.* **133**, 263–282 (2017).
29. Xiao, W., Sohrabi, A. & Seidlits, S. K. Integrating the glioblastoma microenvironment into engineered experimental models. *Future Sci. OA* **3**, FSO189 (2017).
30. Novak, U. & Kaye, A. H. Extracellular matrix and the brain: components and function. *J. Clin. Neurosci.* **7**, 280–290 (2000).
31. Zimmermann, D. R. & Dours-Zimmermann, M. T. Extracellular matrix of the central nervous system: from neglect to challenge. *Histochem. Cell Biol.* **130**, 635–653 (2008).
32. Bertolotto, A., Magrassi, M. L., Orsi, L., Sitia, C. & Schiffer, D. Glycosaminoglycan changes in human gliomas. A biochemical study. *J. Neurooncol.* **4**, 43–48 (1986).
33. Chintala, S. K., Sawaya, R., Gokaslan, Z. L., Fuller, G. & Rao, J. S. Immunohistochemical localization of extracellular matrix proteins in human glioma, both in vivo and in vitro. *Cancer Lett.* **101**, 107–114 (1996).
34. Mahesparan, R. et al. Expression of extracellular matrix components in a highly infiltrative in vivo glioma model. *Acta Neuropathol.* **105**, 49–57 (2003).
35. Cowman, M. K., Lee, H.-G., Schwertfeger, K. L., McCarthy, J. B. & Turley, E. A. The content and size of hyaluronan in biological fluids and tissues. *Front. Immunol.* **6**, 261 (2015).
36. Dicker, K. T. et al. Hyaluronan: A simple polysaccharide with diverse biological functions. *Acta Biomater.* **10**, 1558–1570 (2014).
37. Akiyama, Y. et al. Hyaluronate receptors mediating glioma cell migration and proliferation. *J. Neurooncol.* **53**, 115–127 (2001).
38. Breyer, R. et al. Disruption of intracerebral progression of rat C6 glioblastoma by in vivo treatment with anti-CD44 monoclonal antibody. *J. Neurosurg.* **62**, 140–149 (2000).
39. Ponta, H., Sherman, L. & Herrlich, P. A. CD44: from adhesion molecules to signalling regulators. *Nat. Rev. Mol. Cell Biol.* **4**, 33–45 (2003).
40. Delpech, B. et al. Hyaluronan and hyaluronectin in the extracellular matrix of human brain tumour stroma. *Eur. J. Cancer* **29A**, 1012–1017 (1993).
41. Yoo, K.-C. et al. Proinvasive extracellular matrix remodeling in tumor microenvironment in response to radiation. *Oncogene* **37**, 3317–3328 (2018).
42. Valkonen, M. et al. Elevated expression of hyaluronan synthase 2 associates with decreased survival in diffusely infiltrating astrocytomas. *BMC Cancer* **18**, 664 (2018).
43. Tian, X. et al. High-molecular-mass hyaluronan mediates the cancer resistance of the naked mole rat. *Nature* **499**, 346–349 (2013).
44. Chanmee, T., Ontong, P. & Itano, N. Mini-review. Hyaluronan: a modulator of the tumor microenvironment. *Cancer Lett.* **375**, 20–30 (2016).
45. Chen, J.-W. E. et al. Influence of hyaluronic acid transitions in tumor microenvironment on glioblastoma malignancy and invasive behavior. *Front. Mater* **5**, 39 (2018).
46. Gladson, C. L. The extracellular matrix of gliomas: modulation of cell function. *J. Neuropathol. Exp. Neurol.* **58**, 1029–1040 (1999).
47. Ljubimova, J. Y., Fujita, M., Khazenzon, N. M., Ljubimov, A. V. & Black, K. L. Changes in laminin isoforms associated with brain tumor invasion and angiogenesis. *Front. Biosci.* **11**, 81–88 (2006).
48. Gamble, J. T. et al. Quantification of glioblastoma progression in zebrafish xenografts: Adhesion to laminin alpha 5 promotes glioblastoma microtumor formation and inhibits cell invasion. *Biochem. Biophys. Res. Commun.* **506**, 833–839 (2018).
49. Lathia, J. D. et al. Laminin alpha 2 enables glioblastoma stem cell growth. *Ann. Neurol.* **72**, 766–778 (2012).
50. Lathia, J. D. et al. Integrin alpha 6 regulates glioblastoma stem cells. *Cell Stem Cell* **6**, 421–432 (2010).
51. Shannon, S. et al. Dexamethasone-mediated activation of fibronectin matrix assembly reduces dispersal of primary human glioblastoma cells. *PLoS One* **10**, e0135951 (2015).
52. Serres, E. et al. Fibronectin expression in glioblastomas promotes cell cohesion, collective invasion of basement membrane in vitro and orthotopic tumor growth in mice. *Oncogene* **33**, 3451–3462 (2014).
53. Sabari, J. et al. Fibronectin matrix assembly suppresses dispersal of glioblastoma cells. *PLoS One* **6**, e24810 (2011).
54. Yuan, L. et al. Transglutaminase 2 inhibitor, KCC009, disrupts fibronectin assembly in the extracellular matrix and sensitizes orthotopic glioblastomas to chemotherapy. *Oncogene* **26**, 2563–2573 (2007).
55. Ogawa, K., Oguchi, M., Nakashima, Y. & Yamabe, H. Distribution of collagen Type IV in brain tumors: An immunohistochemical study. *J. Neurooncol.* **7**, 357–366 (1989).
56. Rojiani, A. M. & Dorovini-Zis, K. Glomeruloid vascular structures in glioblastoma multiforme: an immunohistochemical and ultrastructural study. *J. Neurosurg.* **85**, 1078–1084 (1996).
57. Pointer, K. B. et al. Association of collagen architecture with glioblastoma patient survival. *J Neurosurg* **126**, 1812–1821 (2017).
58. Rauch, U. Brain matrix: structure, turnover and necessity. *Biochem. Soc. Trans.* **35**, 656–660 (2007).
59. Lundell, A. et al. Structural basis for interactions between tenascins and lectican C-type lectin domains: evidence for a crosslinking role for tenascins. *Structure* **12**, 1495–1506 (2004).
60. Miroshnikova, Y. A. et al. Tissue mechanics promote IDH1-dependent HIF1α–tenascin C feedback to regulate glioblastoma aggression. *Nat. Cell Biol.* **18**, 1336–1345 (2016).
61. Mirzaei, R. et al. Brain tumor-initiating cells export tenascin-C associated with exosomes to suppress T cell activity. *Oncoimmunology* **7**, e1478647 (2018).
62. Sarkar, S., Nuttall, R. K., Liu, S., Edwards, D. R. & Yong, V. W. Tenascin-C stimulates glioma cell invasion through matrix metalloproteinase-12. *Cancer Res.* **66**, 11771–11780 (2006).
63. Rascher, G. et al. Extracellular matrix and the blood–brain barrier in glioblastoma multiforme: spatial segregation of tenascin and agrin. *Acta Neuropathol.* **104**, 85–91 (2002).
64. Pen, A., Moreno, M. J., Martin, J. & Stanimirovic, D. B. Molecular markers of extracellular matrix remodeling in glioblastoma vessels: microarray study of laser-captured glioblastoma vessels. *Glia* **55**, 559–572 (2007).
65. Pietras, A. et al. Osteopontin-CD44 signaling in the glioma perivascular niche enhances cancer stem cell phenotypes and promotes aggressive tumor growth. *Cell Stem Cell* **14**, 357–369 (2014).
66. Wei, J. et al. Osteopontin mediates glioblastoma-associated macrophage infiltration and is a potential therapeutic target. *J. Clin. Invest.* **129**, 137–149 (2018).
67. Lamour, V. et al. Targeting osteopontin suppresses glioblastoma stem-like cell character and tumorigenicity in vivo. *Int. J. Cancer* **137**, 1047–1057 (2015).
68. Oyinlade, O. et al. Targeting UDP-α-d-glucose 6-dehydrogenase inhibits glioblastoma growth and migration. *Oncogene* **37**, 2615–2629 (2018).
69. Chauvet, D. et al. In vivo measurement of brain tumor elasticity using intraoperative shear wave elastography. *Eur. J. Ultrasound* **37**, 584–590 (2015).
70. Stewart, D. C., Rubiano, A., Dyson, K. & Simmons, C. S. Mechanical characterization of human brain tumors from patients and comparison to potential surgical phantoms. *PLoS One* **12**, e0177561 (2017).
71. Ciasca, G. et al. Nano-mechanical signature of brain tumours. *Nanoscale* **8**, 19629–19643 (2016).
72. Ulrich, T. A. et al. The mechanical rigidity of the extracellular matrix regulates the structure, motility, and proliferation of glioma cells. *Cancer Res.* **69**, 4167–4174 (2009).
73. Thomas, T. W. & DiMilla, P. A. Spreading and motility of human glioblastoma cells on sheets of silicone rubber depend on substratum compliance. *Med. Biol. Eng. Comput.* **38**, 360–370 (2000).
74. Grundy, T. J. et al. Differential response of patient-derived primary glioblastoma cells to environmental stiffness. *Sci. Rep.* **6**, 23353 (2016).
75. Wong, S. Y. et al. Constitutive activation of myosin-dependent contractility sensitizes glioma tumor-initiating cells to mechanical inputs and reduces tissue invasion. *Cancer Res.* **75**, 1113–1122 (2015).
76. Ruiz-Ontañon, P. et al. Cellular plasticity confers migratory and invasive advantages to a population of glioblastoma-initiating cells that infiltrate peritumoral tissue. *Stem Cells* **31**, 1075–1085 (2013).
77. Kim, Y. & Kumar, S. CD44-mediated adhesion to hyaluronic acid contributes to mechanosensing and invasive motility. *Mol. Cancer Res.* **12**, 1416–1429 (2014).
78. Umesh, V., Rape, A. D., Ulrich, T. A. & Kumar, S. Microenvironmental stiffness enhances glioma cell proliferation by stimulating epidermal growth factor receptor signaling. *PLoS One* **9**, e101771 (2014).
79. Mammoto, T. et al. Role of collagen matrix in tumor angiogenesis and glioblastoma multiforme progression. *Am. J. Pathol.* **183**, 1293–1305 (2013).
80. Seano, G. et al. Solid stress in brain tumours causes neuronal loss and neurological dysfunction and can be reversed by lithium. *Nat. Biomed. Eng.* **3**, 230–245 (2019).
81. Watkins, S. et al. Disruption of astrocyte–vascular coupling and the blood–brain barrier by invading glioma cells. *Nat. Commun.* **5**, 4196 (2014).
82. Candiello, J. et al. Biomechanical properties of native basement membranes. *FEBS J.* **274**, 2897–2908 (2007).
83. Charles, N. & Holland, E. C. The perivascular niche microenvironment in brain tumor progression. *Cell Cycle* **9**, 3012–3021 (2010).
84. Giese, A. et al. Migration of human glioma cells on myelin. *Neurosurg.* **38**, 755–764 (1996).
85. Hensel, T., Amberger, V. & Schwab, M. A metalloprotease activity from C6 glioma cells inactivates the myelin-associated neurite growth inhibitors and can be neutralized by antibodies. *Br. J. Cancer* **78**, 1564–1572 (1998).
86. Amberger, V. R., Hensel, T., Ogata, N. & Schwab, M. E. Spreading and migration of human glioma and rat C6 cells on central nervous system myelin in vitro is correlated with tumor malignancy and involves a metalloproteolytic activity. *Cancer Res.* **58**, 149–158 (1998).
87. Oellers, P., Schröer, U., Senner, V., Paulus, W. & Thanos, S. ROCKs are expressed in brain tumors and are required for glioma-cell migration on myelinated axons. *Glia* **57**, 499–509 (2009).
88. Wang, J. et al. Invasion of white matter tracts by glioma stem cells is regulated by a NOTCH1–SOX2 positive-feedback loop. *Nat. Neurosci.* **22**, 91–105 (2019).
89. Balzer, E. M. et al. Physical confinement alters tumor cell adhesion and migration phenotypes. *FASEB J.* **26**, 4045–4056 (2012).
90. Monzo, P. et al. Mechanical confinement triggers glioma linear migration dependent on formin FHOD3. *Mol. Biol. Cell* **27**, 1246–1261 (2016).
91. Heldin, C.-H., Rubin, K., Pietras, K., Ostman, A. & Östman, A. High interstitial fluid pressure — an obstacle in cancer therapy. *Nat. Rev. Cancer* **4**, 806–813 (2004).
92. Swartz, M. A. & Fleury, M. E. Interstitial flow and its effects in soft tissues. *Annu. Rev. Biomed. Eng.* **9**, 229–256 (2007).
93. Abbott, N. J. Evidence for bulk flow of brain interstitial fluid: significance for physiology and pathology. *Neurochem. Int.* **45**, 545–552 (2004).
94. Geer, C. P. & Grossman, S. A. Interstitial fluid flow along white matter tracts: A potentially important mechanism for the dissemination of primary brain tumors. *J. Neurooncol.* **32**, 193–201 (1997).
95. Kingsmore, K. M. et al. Interstitial flow differentially increases patient-derived glioblastoma stem cell invasion *via* CXCR4, CXCL12, and CD44-mediated mechanisms. *Integr. Biol.* **8**, 1246–1260 (2016).
96. Munson, J. M., Bellamkonda, R. V. & Swartz, M. A. Interstitial flow in a 3D microenvironment increases glioma invasion by a CXCR4-dependent mechanism. *Cancer Res.* **73**, 1536–1546 (2013).
97. Cornelison, R. C., Brennan, C. E., Kingsmore, K. M. & Munson, J. M. Convective forces increase CXCR4-dependent glioblastoma cell invasion in GL261 murine model. *Sci. Rep.* **8**, 17057 (2018).
98. Monteiro, A., Hill, R., Pilkington, G. & Madureira, P. The role of hypoxia in glioblastoma invasion. *Cells* **6**, 45 (2017).
99. Lee, C. G. et al. Anti-vascular endothelial growth factor treatment augments tumor radiation response under

normoxic or hypoxic conditions. *Cancer Res.* **60**, 5565–5570 (2000).
100. Figueroa, J. et al. Exosomes from glioma-associated mesenchymal stem cells increase the tumorigenicity of glioma stem-like cells via transfer of miR-1587. *Cancer Res.* **77**, 5808–5819 (2017).
101. Hossain, A. et al. Mesenchymal stem cells isolated from human gliomas increase proliferation and maintain stemness of glioma stem cells through the IL-6/gp130/STAT3 pathway. *Stem Cells* **33**, 2400–2415 (2015).
102. Brandao, M., Simon, T., Critchley, G. & Giamas, G. Astrocytes, the rising stars of the glioblastoma microenvironment. *Glia* **67**, 779–790 (2019).
103. Poon, C. C., Sarkar, S., Yong, V. W. & Kelly, J. J. P. Glioblastoma-associated microglia and macrophages: targets for therapies to improve prognosis. *Brain* **140**, 1548–1560 (2017).
104. Hambardzumyan, D., Gutmann, D. H. & Kettenmann, H. The role of microglia and macrophages in glioma maintenance and progression. *Nat. Neurosci.* **19**, 20–27 (2016).
105. Venkatesh, H. S. et al. Neuronal activity promotes glioma growth through neuroligin-3 secretion. *Cell* **161**, 803–816 (2015).
106. Infanger, D. W. et al. Glioblastoma stem cells are regulated by interleukin-8 signaling in a tumoral perivascular niche. *Cancer Res.* **73**, 7079–7089 (2013).
107. Soda, Y. et al. Transdifferentiation of glioblastoma cells into vascular endothelial cells. *Proc. Natl. Acad. Sci. USA* **108**, 4274–4280 (2011).
108. Hardee, M. E. & Zagzag, D. Mechanisms of glioma-associated neovascularization. *Am. J. Pathol.* **181**, 1126–1141 (2012).
109. Davis, M. E. Glioblastoma: overview of disease and treatment. *Clin. J. Oncol. Nurs.* **20**, S2–S8 (2016).
110. Brat, D. J. et al. Pseudopalisades in glioblastoma are hypoxic, express extracellular matrix proteases, and are formed by an actively migrating cell population. *Cancer Res.* **64**, 920–927 (2004).
111. Lim, S. et al. Glioblastoma-secreted soluble CD44 activates tau pathology in the brain. *Exp. Mol. Med.* **50**, 5 (2018).
112. Lacroix, M. et al. A multivariate analysis of 416 patients with glioblastoma multiforme: prognosis, extent of resection, and survival. *J. Neurosurg.* **95**, 190–198 (2001).
113. Shinoda, J. et al. Fluorescence-guided resection of glioblastoma multiforme by using high-dose fluorescein sodium. *J. Neurosurg.* **99**, 597–603 (2003).
114. Bregy, A. et al. The role of Gliadel wafers in the treatment of high-grade gliomas. *Expert Rev. Anticancer Ther.* **13**, 1453–1461 (2013).
115. Perry, J., Chambers, A., Spithoff, K. & Laperriere, N. Gliadel wafers in the treatment of malignant glioma: a systematic review. *Curr. Oncol.* **14**, 189–194 (2007).
116. Stupp, R. et al. Effect of tumor-treating fields plus maintenance temozolomide vs maintenance temozolomide alone on survival in patients with glioblastoma. *JAMA* **318**, 2306–2316 (2017).
117. Davies, A. M., Weinberg, U. & Palti, Y. Tumor treating fields: a new frontier in cancer therapy. *Ann. N. Y. Acad. Sci.* **1291**, 86–95 (2013).
118. Calabrese, C. et al. A perivascular niche for brain tumor stem cells. *Cancer Cell* **11**, 69–82 (2007). **This paper demonstrated that interactions between endothelial cells and GSCs regulate the self-renewal and tumour-initiating capacity of GSCs, therefore acting as a perivascular niche**.
119. Borovski, T., De Sousa E Melo, F., Vermeulen, L. & Medema, J. P. Cancer stem cell niche: the place to be. *Cancer Res.* **71**, 634–639 (2011).
120. Silver, D. J. & Lathia, J. D. Revealing the glioma cancer stem cell interactome, one niche at a time. *J. Pathol.* **244**, 260–264 (2018).
121. Brooks, M. D., Sengupta, R., Snyder, S. C. & Rubin, J. B. Hitting them where they live: targeting the glioblastoma perivascular stem cell niche. *Curr. Pathobiol. Rep.* **1**, 101–110 (2013).
122. Shiraki, Y. et al. Significance of perivascular tumour cells defined by CD109 expression in progression of glioma. *J. Pathol.* **243**, 468–480 (2017).
123. Wolf, K. J., Lee, S. & Kumar, S. A 3D topographical model of parenchymal infiltration and perivascular invasion in glioblastoma. *APL Bioeng.* **2**, 031903 (2018).
124. Ngo, M. T. & Harley, B. A. C. Perivascular signals alter global gene expression profile of glioblastoma and response to temozolomide in a gelatin hydrogel. *Biomater.* **198**, 122–134 (2019).
125. Zhu, T. S. et al. Endothelial cells create a stem cell niche in glioblastoma by providing NOTCH ligands that nurture self-renewal of cancer stem-like cells. *Cancer Res.* **71**, 6061–6072 (2011).
126. Bao, S. et al. Stem cell-like glioma cells promote tumor angiogenesis through vascular endothelial growth factor. *Cancer Res.* **66**, 7843–7848 (2006).
127. Charles, N. et al. Perivascular nitric oxide activates notch signaling and promotes stem-like character in PDGF-induced glioma cells. *Cell Stem Cell* **6**, 141–152 (2010).
128. Tilghman, J. et al. HMMR maintains the stemness and tumorigenicity of glioblastoma stem-like cells. *Cancer Res.* **74**, 3168–3179 (2014).
129. Chanmee, T., Ontong, P., Kimata, K. & Itano, N. Key roles of hyaluronan and its CD44 receptor in the stemness and survival of cancer stem cells. *Front. Oncol.* **5**, 180 (2015).
130. Ferrandez, E., Gutierrez, O., Segundo, D. S. & Fernandez-Luna, J. L. NFκB activation in differentiating glioblastoma stem-like cells is promoted by hyaluronic acid signaling through TLR4. *Sci. Rep.* **8**, 6341 (2018).
131. Chen, J. & Kumar, S. Biophysical regulation of cancer stem/initiating cells: Implications for disease mechanisms and translation. *Curr. Opin. Biomed. Eng.* **1**, 87–95 (2017).
132. Barnes, J. M. et al. A tension-mediated glycocalyx–integrin feedback loop promotes mesenchymal-like glioblastoma. *Nat. Cell Biol.* **20**, 1203–1214 (2018).
133. Iwadate, Y. Epithelial–mesenchymal transition in glioblastoma progression. *Oncol. Lett.* **11**, 1615–1620 (2016).
134. Lau, J. et al. STAT3 blockade inhibits a radiation-induced proneural-to-mesenchymal transition in glioma. *Cancer Res.* **75**, 4302–4311 (2015).
135. Bhat, K. P. L. et al. Mesenchymal differentiation mediated by NF-κB promotes radiation resistance in glioblastoma. *Cancer Cell* **24**, 331–346 (2013).
136. Xiao, W. et al. Brain-mimetic 3D culture platforms allow investigation of cooperative effects of extracellular matrix features on therapeutic resistance in glioblastoma. *Cancer Res.* **78**, 1358–1370 (2018).
137. Soeda, A. et al. Hypoxia promotes expansion of the CD133-positive glioma stem cells through activation of HIF-1α. *Oncogene* **28**, 3949–3959 (2009).
138. Colwell, N. et al. Hypoxia in the glioblastoma microenvironment: shaping the phenotype of cancer stem-like cells. *Neuro. Oncol.* **19**, 887–896 (2017).
139. Heddleston, J. M., Li, Z., McLendon, R. E., Hjelmeland, A. B. & Rich, J. N. The hypoxic microenvironment maintains glioblastoma stem cells and promotes reprogramming towards a cancer stem cell phenotype. *Cell Cycle* **8**, 3274–3284 (2009).
140. Gupta, K. & Burns, T. C. Radiation-induced alterations in the recurrent glioblastoma microenvironment: therapeutic implications. *Front. Oncol.* **8**, 503 (2018).
141. Bao, S. et al. Glioma stem cells promote radioresistance by preferential activation of the DNA damage response. *Nature* **444**, 756–760 (2006).
142. Rath, B. H., Wahba, A., Camphausen, K. & Tofilon, P. J. Coculture with astrocytes reduces the radiosensitivity of glioblastoma stem-like cells and identifies additional targets for radiosensitization. *Cancer Med.* **4**, 1705–1716 (2015).
143. De Pascalis, I. et al. Endothelial trans-differentiation in glioblastoma recurring after radiotherapy. *Mod. Pathol.* **31**, 1361–1366 (2018).
144. Mao, L. et al. Enhancement of invadopodia activity in glioma cells by sublethal doses of irradiation and temozolomide. *J. Neurosurg.* **129**, 598–610 (2018).
145. Tsidulko, A. Y. et al. Conventional anti-glioblastoma chemotherapy affects proteoglycan composition of brain extracellular matrix in rat experimental model in vivo. *Front. Pharmacol.* **9**, 1104 (2018).
146. Yoshida, D., Piepmeier, J. M., Bergenheim, T., Henriksson, R. & Teramoto, A. Suppression of matrix metalloproteinase-2-mediated cell invasion in U87MG, human glioma cells by anti-microtubule agent: in vitro study. *Br. J. Cancer* **77**, 21–25 (1998).
147. Sawyers, C. Targeted cancer therapy. *Nature* **432**, 294–297 (2004).
148. Higgins, M. J. & Baselga, J. Targeted therapies for breast cancer. *J. Clin. Invest.* **121**, 3797–3803 (2011).
149. Westphal, M., Maire, C. L. & Lamszus, K. EGFR as a target for glioblastoma treatment: an unfulfilled promise. *CNS Drugs* **31**, 723–735 (2017).
150. Butowski, N. et al. Orally administered colony stimulating factor 1 receptor inhibitor PLX3397 in recurrent glioblastoma: an ivy foundation early phase clinical trials consortium phase II study. *Neuro. Oncol.* **18**, 557–564 (2016).
151. Friedman, H. S. et al. Bevacizumab alone and in combination with irinotecan in recurrent glioblastoma. *J. Clin. Oncol.* **27**, 4733–4740 (2009).
152. Kreisl, T. N. et al. Phase II trial of single-agent bevacizumab followed by bevacizumab plus irinotecan at tumor progression in recurrent glioblastoma. *J. Clin. Oncol.* **27**, 740–745 (2009).
153. Wenger, K. J. et al. Bevacizumab as a last-line treatment for glioblastoma following failure of radiotherapy, temozolomide and lomustine. *Oncol. Lett.* **14**, 1141–1146 (2017).
154. Pàez-Ribes, M. et al. Antiangiogenic therapy elicits malignant progression of tumors to increased local invasion and distant metastasis. *Cancer Cell* **15**, 220–231 (2009).
155. Momeny, M. et al. Blockade of vascular endothelial growth factor receptors by tivozanib has potential anti-tumour effects on human glioblastoma cells. *Sci. Rep.* **7**, 44075 (2017).
156. Batchelor, T. T. et al. Phase II study of cediranib, an oral pan-vascular endothelial growth factor receptor tyrosine kinase inhibitor, in patients with recurrent glioblastoma. *J. Clin. Oncol.* **28**, 2817–2823 (2010).
157. Batchelor, T. T. et al. Phase III randomized trial comparing the efficacy of cediranib as monotherapy, and in combination with lomustine, versus lomustine alone in patients with recurrent glioblastoma. *J. Clin. Oncol.* **31**, 3212–3218 (2013).
158. Kreisl, T. N. et al. Continuous daily sunitinib for recurrent glioblastoma. *J. Neurooncol.* **111**, 41–48 (2013).
159. Neal, J. & Wakelee, H. AMG-386, a selective angiopoietin-1/-2-neutralizing peptibody for the potential treatment of cancer. *Curr. Opin. Mol. Ther.* **12**, 487–495 (2010).
160. Reardon, D. A. et al. A review of VEGF/VEGFR-targeted therapeutics for recurrent glioblastoma. *J. Natl. Compr. Canc. Netw.* **9**, 414–427 (2011).
161. Fang, H. & DeClerck, Y. A. Targeting the tumor microenvironment: from understanding pathways to effective clinical trials. *Cancer Res.* **73**, 4965–4977 (2013).
162. Papadopoulos, K. P. et al. A phase 1 open-label, accelerated dose-escalation study of the hypoxia-activated prodrug AQ4N in patients with advanced malignancies. *Clin. Cancer Res.* **14**, 7110–7115 (2008).
163. Albertella, M. R. et al. Hypoxia-selective targeting by the bioreductive prodrug AQ4N in patients with solid tumors: results of a phase I study. *Clin. Cancer Res.* **14**, 1096–1104 (2008).
164. Patterson, L. H. & McKeown, S. R. AQ4N: a new approach to hypoxia-activated cancer chemotherapy. *Br. J. Cancer* **83**, 1589–1593 (2000).
165. Jain, K. K. A critical overview of targeted therapies for glioblastoma. *Front. Oncol.* **8**, 419 (2018).
166. Carbonell, W. S., DeLay, M., Jahangiri, A., Park, C. C. & Aghi, M. K. β1 integrin targeting potentiates antiangiogenic therapy and inhibits the growth of bevacizumab-resistant glioblastoma. *Cancer Res.* **73**, 3145–3154 (2013).
167. Scaringi, C., Minniti, G., Caporello, P. & Enrici, R. M. Integrin inhibitor cilengitide for the treatment of glioblastoma: a brief overview of current clinical results. *Anticancer. Res.* **32**, 4213–4223 (2012).
168. Stupp, R. et al. Cilengitide combined with standard treatment for patients with newly diagnosed glioblastoma with methylated MGMT promoter (CENTRIC EORTC 26071-22072 study): a multicentre, randomised, open-label, phase 3 trial. *Lancet Oncol.* **15**, 1100–1108 (2014).
169. Tucci, M., Stucci, S. & Silvestris, F. Does cilengitide deserve another chance? *Lancet. Oncol.* **15**, e584–e585 (2014).
170. Vogelbaum, M. A. & Aghi, M. K. Convection-enhanced delivery for the treatment of glioblastoma. *Neuro. Oncol.* **17**, ii3–ii8 (2015).
171. Brown, M. C. et al. Cancer immunotherapy with recombinant poliovirus induces IFN-dominant activation of dendritic cells and tumor antigen-specific CTLs. *Sci. Transl. Med.* **9**, eaan4220 (2017).
172. Desjardins, A. et al. Recurrent glioblastoma treated with recombinant poliovirus. *N. Engl. J. Med.* **379**, 150–161 (2018).
173. Rape, A., Ananthanarayanan, B. & Kumar, S. Engineering strategies to mimic the glioblastoma microenvironment. *Adv. Drug Deliv. Rev.* **79–80**, 172–183 (2014).
174. Stylli, S. S., Luwor, R. B., Ware, T. M. B., Tan, F. & Kaye, A. H. Mouse models of glioma. *J. Clin. Neurosci.* **22**, 619–626 (2015).

175. Joo, K. M. et al. Patient-specific orthotopic glioblastoma xenograft models recapitulate the histopathology and biology of human glioblastomas in situ. *Cell Rep.* **3**, 260–273 (2013).
176. Simeonova, I. & Huillard, E. In vivo models of brain tumors: roles of genetically engineered mouse models in understanding tumor biology and use in preclinical studies. *Cell. Mol. Life Sci.* **71**, 4007–4026 (2014).
177. Ismail Kola, J. L. Can the pharmaceutical industry reduce attrition rates? *Nat. Rev. Drug Discov.* **3**, 711–715 (2004).
178. Wu, M. & Swartz, M. A. Modeling tumor microenvironments in vitro. *J. Biomech. Eng.* **136**, 021011 (2014).
179. Pathak, A. & Kumar, S. Independent regulation of tumor cell migration by matrix stiffness and confinement. *Proc. Natl. Acad. Sci. USA* **109**, 10334–10339 (2012).
180. Diao, W. et al. Behaviors of glioblastoma cells in in vitro microenvironments. *Sci. Rep.* **9**, 85 (2019).
181. Fernandez-Fuente, G., Mollinedo, P., Grande, L., Vazquez-Barquero, A. & Fernandez-Luna, J. L. Culture dimensionality influences the resistance of glioblastoma stem-like cells to multikinase inhibitors. *Mol. Cancer Ther.* **13**, 1664–1672 (2014).
182. Rape, A. D., Zibinsky, M., Murthy, N. & Kumar, S. A synthetic hydrogel for the high-throughput study of cell–ECM interactions. *Nat. Commun.* **6**, 8129 (2015).
183. Ananthanarayanan, B., Kim, Y. & Kumar, S. Elucidating the mechanobiology of malignant brain tumors using a brain matrix–mimetic hyaluronic acid hydrogel platform. *Biomater.* **32**, 7913–7923 (2011).
184. Wolf, K. J. & Kumar, S. Hyaluronic acid: incorporating the bio into the material. *ACS Biomater. Sci. Eng.* [epub ahead of print], (2019).
185. Schanté, C. E., Zuber, G., Herlin, C. & Vandamme, T. F. Chemical modifications of hyaluronic acid for the synthesis of derivatives for a broad range of biomedical applications. *Carbohydr. Polym.* **85**, 469–489 (2011).
186. Kaphle, P., Li, Y. & Yao, L. The mechanical and pharmacological regulation of glioblastoma cell migration in 3D matrices. *J. Cell. Physiol.* **234**, 3948–3960 (2019).
187. Ulrich, T. A., Jain, A., Tanner, K., MacKay, J. L. & Kumar, S. Probing cellular mechanobiology in three-dimensional culture with collagen–agarose matrices. *Biomater.* **31**, 1875–1884 (2010).
188. Ulrich, T. A., Lee, T. G., Shon, H. K., Moon, D. W. & Kumar, S. Microscale mechanisms of agarose-induced disruption of collagen remodeling. *Biomater.* **32**, 5633–5642 (2011).
189. Yang, Y. et al. Influence of chondroitin sulfate and hyaluronic acid on structure, mechanical properties, and glioma invasion of collagen I gels. *Biomater.* **32**, 7932–7940 (2011).
190. Yang, Y., Motte, S. & Kaufman, L. J. Pore size variable type I collagen gels and their interaction with glioma cells. *Biomater.* **31**, 5678–5688 (2010).
191. Ylivinkka, I. et al. Motility of glioblastoma cells is driven by netrin-1 induced gain of stemness. *J. Exp. Clin. Cancer Res.* **36**, 9 (2017).
192. Kumar, K. K. et al. Glioma stem cell invasion through regulation of the interconnected ERK, integrin α 6 and N-cadherin signaling pathway. *Cell. Signal.* **24**, 2076–2084 (2012).
193. Wang, C., Tong, X., Jiang, X. & Yang, F. Effect of matrix metalloproteinase-mediated matrix degradation on glioblastoma cell behavior in 3D PEG-based hydrogels. *J. Biomed. Mater. Res. A* **105**, 770–778 (2017).
194. Ma, N. K. L. et al. Collaboration of 3D context and extracellular matrix in the development of glioma stemness in a 3D model. *Biomater.* **78**, 62–73 (2016).
195. Martínez-Ramos, C. & Lebourg, M. Three-dimensional constructs using hyaluronan cell carrier as a tool for the study of cancer stem cells. *J. Biomed. Mater. Res. B Appl. Biomater.* **103**, 1249–1257 (2015).
196. Heffernan, J. M. et al. PNIPAAm-co-Jeffamine® (PNJ) scaffolds as in vitro models for niche enrichment of glioblastoma stem-like cells. *Biomater.* **143**, 149–158 (2017).
197. Kievit, F. M. et al. Modeling the tumor microenvironment using chitosan-alginate scaffolds to control the stem-like state of glioblastoma cells. *Biomater. Sci.* **4**, 610–613 (2016).
198. Koh, I. et al. The mode and dynamics of glioblastoma cell invasion into a decellularized tissue-derived extracellular matrix-based three-dimensional tumor model. *Sci. Rep.* **8**, 4608 (2018).
199. Yi, H.-G. et al. A bioprinted human-glioblastoma-on-a-chip for the identification of patient-specific responses to chemoradiotherapy. *Nat. Biomed. Eng.* [epub ahead of print], (2019).
This paper describes a 3D-printed, spatially organized model of perivascular invasion that includes brain-derived matrix and patient-derived tumour cells.
200. Weiswald, L.-B., Bellet, D. & Dangles-Marie, V. Spherical cancer models in tumor biology. *Neoplasia* **17**, 1–15 (2015).
201. Lee, J. et al. Tumor stem cells derived from glioblastomas cultured in bFGF and EGF more closely mirror the phenotype and genotype of primary tumors than do serum-cultured cell lines. *Cancer Cell* **9**, 391–403 (2006).
202. Timmins, N. E. & Nielsen, L. K. Generation of multicellular tumor spheroids by the hanging-drop method. *Methods Mol. Med.* **140**, 141–151 (2007).
203. Mirab, F., Kang, Y. J. & Majd, S. Preparation and characterization of size-controlled glioma spheroids using agarose hydrogel microwells. *PLoS One* **14**, e0211078 (2019).
204. Zhang, X.-P. et al. Notch activation promotes cell proliferation and the formation of neural stem cell-like colonies in human glioma cells. *Mol. Cell. Biochem.* **307**, 101–108 (2007).
205. Herrera-Perez, R. M. et al. Presence of stromal cells in a bioengineered tumor microenvironment alters glioblastoma migration and response to STAT3 inhibition. *PLoS One* **13**, e0194183 (2018).
206. Florczyk, S. J. et al. Porous chitosan–hyaluronic acid scaffolds as a mimic of glioblastoma microenvironment ECM. *Biomaterials* **34**, 10143–10150 (2013).
207. Herrera-Perez, M., Voytik-Harbin, S. L. & Rickus, J. L. Extracellular matrix properties regulate the migratory response of glioblastoma stem cells in three-dimensional culture. *Tissue Eng. Part A* **21**, 2572–2582 (2015).
208. Pedron, S., Becka, E. & Harley, B. A. C. C. Regulation of glioma cell phenotype in 3D matrices by hyaluronic acid. *Biomaterials* **34**, 7408–7417 (2013).
209. Wang, C., Tong, X. & Yang, F. Bioengineered 3D brain tumor model to elucidate the effects of matrix stiffness on glioblastoma cell behavior using PEG-based hydrogels. *Mol. Pharm.* **11**, 2115–2125 (2014).
210. Heffernan, J. M., Overstreet, D. J., Le, L. D., Vernon, B. L. & Sirianni, R. W. Bioengineered scaffolds for 3D analysis of glioblastoma proliferation and invasion. *Ann. Biomed. Eng.* **43**, 1965–1977 (2014).
211. Pedron, S., Hanselman, J. S., Schroeder, M. A., Sarkaria, J. N. & Harley, B. A. C. Extracellular hyaluronic acid influences the efficacy of EGFR tyrosine kinase inhibitors in a biomaterial model of glioblastoma. *Adv. Healthc. Mater.* **6**, 1700529 (2017).
212. Pedron, S. et al. Hyaluronic acid-functionalized gelatin hydrogels reveal extracellular matrix signals temper the efficacy of erlotinib against patient-derived glioblastoma specimens. *Biomaterials* **219**, 119371 (2019).
213. Shin, H. Fabrication methods of an engineered microenvironment for analysis of cell–biomaterial interactions. *Biomaterials* **28**, 126–133 (2007).
214. Brown, T. E. & Anseth, K. S. Spatiotemporal hydrogel biomaterials for regenerative medicine. *Chem. Soc. Rev.* **46**, 6532–6552 (2017).
215. Cortese, B., Gigli, G. & Riehle, M. Mechanical gradient cues for guided cell motility and control of cell behavior on uniform substrates. *Adv. Funct. Mater.* **19**, 2961–2968 (2009).
216. Pedron, S., Becka, E. & Harley, B. A. Spatially gradated hydrogel platform as a 3D engineered tumor microenvironment. *Adv. Mater.* **27**, 1567–1572 (2015).
A microfluidic-based mixing tool was developed and applied to generate 3D materials with gradients of matrix and cellular composition, facilitating rapid investigation of TME parameters on tumour progression.
217. Rao, S. S. et al. Inherent interfacial mechanical gradients in 3D hydrogels influence tumor cell behaviors. *PLoS One* **7**, e35852 (2012).
218. Pedron, S. & Harley, B. A. C. Impact of the biophysical features of a 3D gelatin microenvironment on glioblastoma malignancy. *J. Biomed. Mater. Res. A* **101**, 3404–3415 (2013).
219. Gritsenko, P., Leenders, W. & Friedl, P. Recapitulating in vivo-like plasticity of glioma cell invasion along blood vessels and in astrocyte-rich stroma. *Histochem. Cell Biol.* **148**, 1–12 (2017).
220. Rape, A. D. & Kumar, S. A composite hydrogel platform for the dissection of tumor cell migration at tissue interfaces. *Biomaterials* **35**, 8846–8853 (2014).
221. Beliveau, A., Thomas, G., Gong, J., Wen, Q. & Jain, A. Aligned nanotopography promotes a migratory state in glioblastoma multiforme tumor cells. *Sci. Rep.* **6**, 26143 (2016).
222. Kievit, F. M. et al. Aligned chitosan–polycaprolactone polyblend nanofibers promote the migration of glioblastoma cells. *Adv. Healthc. Mater.* **2**, 1651–1659 (2013).
223. Sharma, P., Sheets, K., Elankumaran, S. & Nain, A. S. The mechanistic influence of aligned nanofibers on cell shape, migration and blebbing dynamics of glioma cells. *Integr. Biol.* **5**, 1036–1044 (2013).
224. Grodecki, J. et al. Glioma–astrocyte interactions on white matter tract–mimetic aligned electrospun nanofibers. *Biotechnol. Prog.* **31**, 1406–1415 (2015).
225. Rao, S. S. et al. Mimicking white matter tract topography using core–shell electrospun nanofibers to examine migration of malignant brain tumors. *Biomaterials* **34**, 5181–5190 (2013).
226. Agudelo-Garcia, P. A. et al. Glioma cell migration on three-dimensional nanofiber scaffolds is regulated by substrate topography and abolished by inhibition of STAT3 signaling. *Neoplasia* **13**, 831–840 (2011).
227. Sung, K. E. & Beebe, D. J. Microfluidic 3D models of cancer. *Adv. Drug Deliv. Rev.* **79–80**, 68–78 (2014).
228. Ayuso, J. M. et al. Glioblastoma on a microfluidic chip: Generating pseudopalisades and enhancing aggressiveness through blood vessel obstruction events. *Neuro. Oncol.* **19**, 503–513 (2017).
This paper applied a microfluidic model to test how pseudopalisades form, which had previously only been inferred from in vivo data.
229. Truong, D. et al. A three-dimensional (3D) organotypic microfluidic model for glioma stem cells — Vascular interactions. *Biomaterials* **198**, 63–77 (2019).
230. Chonan, Y., Taki, S., Sampetrean, O., Saya, H. & Sudo, R. Endothelium-induced three-dimensional invasion of heterogeneous glioma initiating cells in a microfluidic coculture platform. *Integr. Biol.* **9**, 762–773 (2017).
231. Xiao, Y. et al. Ex vivo dynamics of human glioblastoma cells in a microvasculature-on-a-chip system correlates with tumor heterogeneity and subtypes. *Adv. Sci.* **6**, 1801531 (2019).
232. Akay, M. et al. Drug screening of human GBM spheroids in brain cancer chip. *Sci. Rep.* **8**, 15423 (2018).
233. Han, J. et al. Rapid emergence and mechanisms of resistance by U87 glioblastoma cells to doxorubicin in an in vitro tumor microfluidic ecology. *Proc. Natl. Acad. Sci. USA* **113**, 14283–14288 (2016).
234. Fan, Y. et al. Engineering a brain cancer chip for high-throughput drug screening. *Sci. Rep.* **6**, 25062 (2016).
235. Jie, M. et al. Evaluation of drug combination for glioblastoma based on an intestine–liver metabolic model on microchip. *Analyst* **142**, 3629–3638 (2017).
236. Dai, X., Ma, C., Lan, Q. & Xu, T. 3D bioprinted glioma stem cells for brain tumor model and applications of drug susceptibility. *Biofabrication* **8**, 045005 (2016).
237. Wang, X. et al. Bioprinting of glioma stem cells improves their endotheliogenic potential. *Colloids Surf. B Biointerfaces* **171**, 629–637 (2018).
238. Heinrich, M. A. et al. 3D-Bioprinted mini-brain: a glioblastoma model to study cellular interactions and therapeutics. *Adv. Mater.* **31**, 1806590 (2019).
239. Hubert, C. G. et al. A three-dimensional organoid culture system derived from human glioblastomas recapitulates the hypoxic gradients and cancer stem cell heterogeneity of tumors found in vivo. *Cancer Res.* **76**, 2465–2477 (2016).
The method used in this paper to derive and culture patient cells and matrix minimally disturbed cell–matrix interactions, preserved tumour cell heterogeneity and resulted in an accurate recapitulation of patient tumour response in an orthotopic xenograft culture.
240. Hattori, N. Cerebral organoids model human brain development and microcephaly. *Mov. Disord.* **29**, 185–185 (2014).
241. Nayernia, Z. et al. The relationship between brain tumor cell invasion of engineered neural tissues and in vivo features of glioblastoma. *Biomaterials* **34**, 8279–8290 (2013).
242. Huang, Y., Agrawal, B., Clark, P. A., Williams, J. C. & Kuo, J. S. Evaluation of cancer stem cell migration using compartmentalizing microfluidic devices and live cell imaging. *J. Vis. Exp.* **58**, e3297 (2011).
243. Piccolo, S. R. & Frey, L. J. Clinical and molecular models of glioblastoma multiforme survival. *Int. J. Data Min. Bioinform.* **7**, 245–265 (2013).
244. Verhaak, R. G. W. et al. Integrated genomic analysis identifies clinically relevant subtypes of glioblastoma characterized by abnormalities in PDGFRA, IDH1, EGFR, and NF1. *Cancer Cell* **17**, 98–110 (2010).
245. US National Library of Medicine. *ClinicalTrials.gov* https://clinicaltrials.gov/ct2/show/NCT02060890 (2018).

246. Wang, Y. I., Abaci, H. E. & Shuler, M. L. Microfluidic blood–brain barrier model provides in vivo-like barrier properties for drug permeability screening. *Biotechnol. Bioeng.* **114**, 184–194 (2017).
247. van der Helm, M. W., van der Meer, A. D., Eijkel, J. C. T., van den Berg, A. & Segerink, L. I. Microfluidic organ-on-chip technology for blood–brain barrier research. *Tissue Barriers* **4**, e1142493 (2016).
248. Randazzo, M., Pisapia, J. M., Singh, N. & Thawani, J. P. 3D printing in neurosurgery: A systematic review. *Surg. Neurol. Int.* **7**, S801–S809 (2016).
249. Ploch, C. C., Mansi, C. S. S. A., Jayamohan, J. & Kuhl, E. Using 3D printing to create personalized brain models for neurosurgical training and preoperative planning. *World Neurosurg.* **90**, 668–674 (2016).
250. Naftulin, J. S., Kimchi, E. Y. & Cash, S. S. Streamlined, inexpensive 3D printing of the brain and skull. *PLoS One* **10**, e0136198 (2015).
251. Treiber, J. M. et al. Molecular physiology of contrast enhancement in glioblastomas: an analysis of The Cancer Imaging Archive (TCIA). *J. Clin. Neurosci.* **55**, 86–92 (2018).
252. Gevaert, O. et al. Glioblastoma multiforme: exploratory radiogenomic analysis by using quantitative image features. *Radiology* **273**, 168–174 (2014).
253. Chow, D. et al. Imaging genetic heterogeneity in glioblastoma and other glial tumors: review of current methods and future directions. *Am. J. Roentgenol.* **210**, 30–38 (2018).
254. Lao, J. et al. A deep learning-based radiomics model for prediction of survival in glioblastoma multiforme. *Sci. Rep.* **7**, 10353 (2017).
255. Dupont, C., Betrouni, N., Reyns, N. & Vermandel, M. On image segmentation methods applied to glioblastoma: state of art and new trends. *IRBM* **37**, 131–143 (2016).
256. Tamimi, A. F. & Juweid, M. in *Glioblastoma* Ch. 8 (ed De Vleeschouwer, S.) (Codon Publications, 2017).
257. Lee, J. H. et al. Human glioblastoma arises from subventricular zone cells with low-level driver mutations. *Nature* **560**, 243–247 (2018).
258. Khalifa, J. et al. Subventricular zones: new key targets for glioblastoma treatment. *Radiat. Oncol.* **12**, 67 (2017).
259. Chen, L. et al. Increased subventricular zone radiation dose correlates with survival in glioblastoma patients after gross total resection. *Int. J. Radiat. Oncol.* **86**, 616–622 (2013).
260. Ohgaki, H. & Kleihues, P. Genetic pathways to primary and secondary glioblastoma. *Am. J. Pathol.* **170**, 1445–1453 (2007).
261. Gupta, A. & Dwivedi, T. A simplified overview of World Health Organization classification update of central nervous system tumors 2016. *J. Neurosci. Rural Pract.* **8**, 629–641 (2017).
262. Yan, H. et al. *IDH1* and *IDH2* mutations in gliomas. *N. Engl. J. Med.* **360**, 765–773 (2009).
263. Hartmann, C. et al. Patients with IDH1 wild type anaplastic astrocytomas exhibit worse prognosis than IDH1-mutated glioblastomas, and IDH1 mutation status accounts for the unfavorable prognostic effect of higher age: implications for classification of gliomas. *Acta Neuropathol.* **120**, 707–718 (2010).
264. Wilson, T. A., Karajannis, M. A. & Harter, D. H. Glioblastoma multiforme: state of the art and future therapeutics. *Surg. Neurol. Int.* **5**, 64 (2014).
265. Mutter, N. & Stupp, R. Temozolomide: a milestone in neuro-oncology and beyond? *Expert Rev. Anticancer Ther.* **6**, 1187–1204 (2006).
266. Hegi, M. E. et al. Clinical trial substantiates the predictive value of O-6-methylguanine-DNA methyltransferase promoter methylation in glioblastoma patients treated with temozolomide. *Clin. Cancer Res.* **10**, 1871–1874 (2004).
267. Kappelle, A. C. et al. PCV chemotherapy for recurrent glioblastoma multiforme. *Neurology* **56**, 118–120 (2001).
268. Weller, M., Cloughesy, T., Perry, J. R. & Wick, W. Standards of care for treatment of recurrent glioblastoma — are we there yet? *Neuro. Oncol.* **15**, 4–27 (2013).

Acknowledgements
The authors gratefully acknowledge financial support from the National Science Foundation (Graduate Research Fellowship to K.J.W.) and the National Institutes of Health (Ruth L. Kirschstein Predoctoral Individual National Research Service Award F31CA228317 to K.J.W.; Ruth L. Kirschstein Postdoctoral Individual National Research Service Award F32CA221366 to J.C.; R21EB025017, R01GM122375 and R01DK118940 to S.K.; and R01CA227136 to M.K.A. and S.K.). J.D.C. has received funding from the European Union's Horizon 2020 research and innovation programme under the Marie Skłodowska-Curie grant agreement no. 752097.

Author contributions
K.J.W., J.C. and J.D.C. researched data for the article. K.J.W. and S.K. made substantial contributions to manuscript writing and the discussion of content. All authors reviewed and edited the manuscript before submission.

Competing interests
The authors declare no competing financial interests.